Background

The Indian River Lagoon watershed covers 2,284 square miles, while waters span 353 square miles. 3 distinct lagoons (Mosquito Lagoon, Banana River, Indian River) comprise the 156-mile-long estuary system (width ranging from 0.5-5 miles), brackish in composition (salt water from the Atlantic Ocean mixes with freshwater from slow moving creeks, rivers, and wetlands), with water moving more so due to wind than tidal effects. The hydrology of the region was greatly altered due to the Drainage Acts of Florida (1916), increasing storm water discharge volume into the river. Due to the limited number of outlets, water resides for long periods of time (>1 year; Smith 1993) in parts of the lagoon, resulting in increased nutrient loads from agriculture and urbanization, setting the stage for persistent algal blooms and increased turbidity. Seagrass distribution, area coverage, and health can be thought of as a gauge of the lagoon's overall health (given their sensitivity to water quality changes). A single acre of seagrass may support as many as 40,000 fish and can produce over 10 tons of leaves per year. This is of great interest not only for the IRL, but for waterways in general; the statewide economic benefit of seagrasses collectively yields $55.4 billion annually (IRLNEP, 2020), with the annual economic value of the lagoon was estimated at $3.7 billion in 2007 (SJRWMD, 2020). ◎

Since the superbloom in 2011, extensive seagrass loss has been observed: 52% acreage loss between 2009 to 2017 (Morris, Chamberlain, Jacoby, 2018). The bloom event consists of two concurrent blooms: The lesser of the two restricted to the central IRL, and the "superbloom," which covered approximately 53,000 hecares in BRL, northern IRL, and southern Mosquito Lagoon. IRL Comprehensive Conservation and Management Plan Goals for Fiscal Year 2021 designates seagrass habitats as a Level 1: Critical health concern, defined as "Conditions threatens immediate and long-term prognosis for lagoon health. Indicators are unfavorable. Trend is negative. Immediate and aggressive intervention is urgently needed to stop and reverse trend."

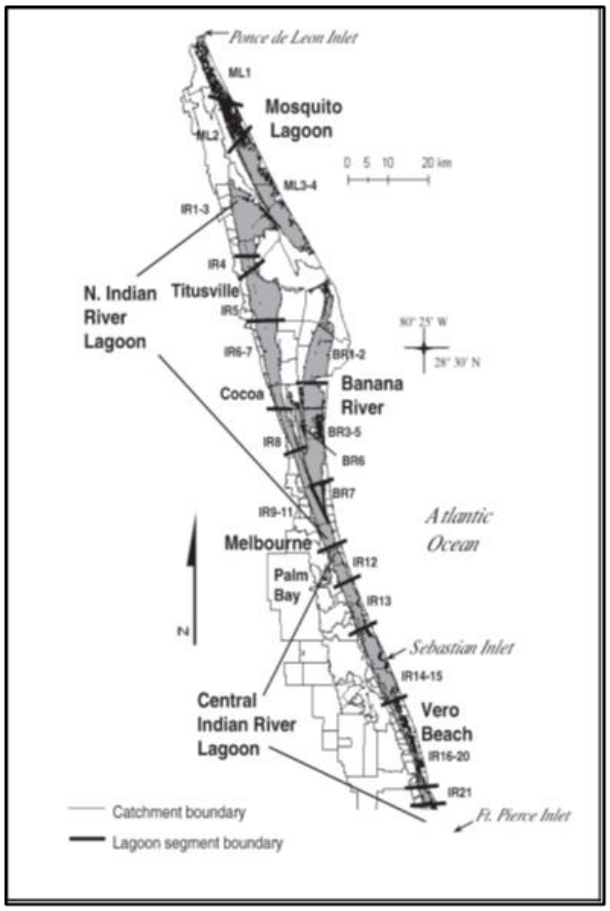

Figure 1: Overall IRL basin boundary+seagrass mangagment areas (Virnstein, Stweard, Morris, 2006)

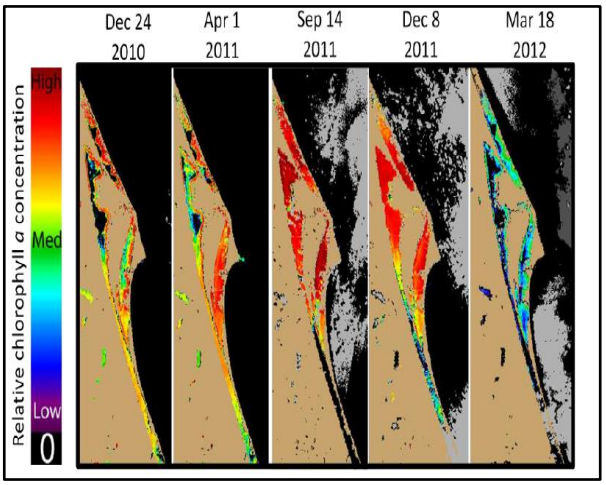

Figure 2: MERIS Satellite images of the Indian River Lagoon system depicting the relative intensity (concentration of chlorophyll) of the 2011 phytoplankton superbloom (SJRWMD, 2012).

Background

Seagrasses can be characterized on their growth forms, which range from small plants (i.e. *Halophila* , *Halodule*) to large plants with thick leaves (i.e. *Thalassia* , *Enhalus* , *Posidonia*). Their local distributions resemble terrestrial grasses (forming monospecific meadows). While no particular structures in seagrass that can be identified as unique in terms of structural adaptation to the marine environment, there is a suite of characteristics that together can be taken as representitive of their morphology:

Strap-shaped leaves and anatomical reinforcement to resist wave action
Adaptation of leaves to carry out photosynthesis in a marine environment
Osmotic adjustment and other adaptations within the leaf blade and leaf sheath
Modifications to rhizome and roots for different substrates
Pollination by hydrophily
Reduction in the layers of pollen wall
Unique features associated with seed formation and dispersal mechanics

Growing conditions are fairly unified: physiological mechanisms have evolved that allow for fluctuations in salinity, and most species have high light requirements (estimate general range 11%-37% surface light (Cussioli et al., 2020). Thus, increasing turbidity (sediment resuspension, anthropogenic factors) leads to decrease in seagrass growth and abundance.

In contrast to the lack of unique morphological adaptations, several specialized physiological mechanisms have evolved over time: for example, in vascular land plants, stomata act as a control system for the movement of CO_2 (in/out) and water vapor (out). Seagrasses have evolved away from developing this structure (so much so that genes for stomata have been shown to have been removed from the genome of species such as *Z. marina* (Olsen, Rouzé, Cerhelst, 2016)). Presumably the adaptation arose as a consequence of living underwater: gaseous movement in a liquid medium vs gasesous medium draws a stark comparison (rates of diffusion in gas are reduced considerably). Instead, gas exchange occurs through permeable cuticles (polyester-based protective structure, forms as a multi-layered lipid structure on outermost surface of organ in continuation with the cell wall), while seagrass roots and rhizomes have aerenchyma to facilitate gas transport. This adaptation (loss of stomata), extreme reduction of cuticle, and leaf epidermis convertion into the primary site of photosynthesis represent the photosynthetic adaptation to the marine environment.

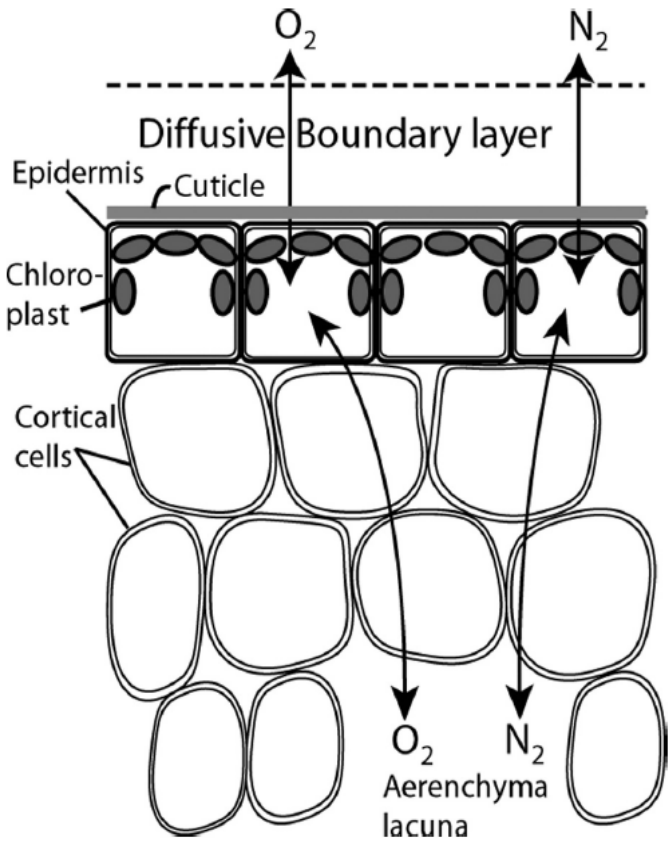

Figure : Pathways of gaseous movenent in photosynthetic and aerenchymal tissue of seagrass leaves (Larkum, Drew, Ralph, 2006).

Background

Catagorically, seagrasses form an ecological group (as opposed to a taxonomic group), implying the different seagrass families do not have to be closely related (Larkum, Kendrick, Ralph, 2018). Clarifying the taxonomy is challenging; there are no morphological characteristics that readily distinguish seagrasses from other aquatic plants (Papenbrock, 2012), and coupled with high phenotypic plasticity (Larkum, Orth, Duarte, 2007), the best option would appear to be using molecular methods. In an attempt to better understand the evolutionary history and relationships of seagrasses, bioinformatic analysis was performed.

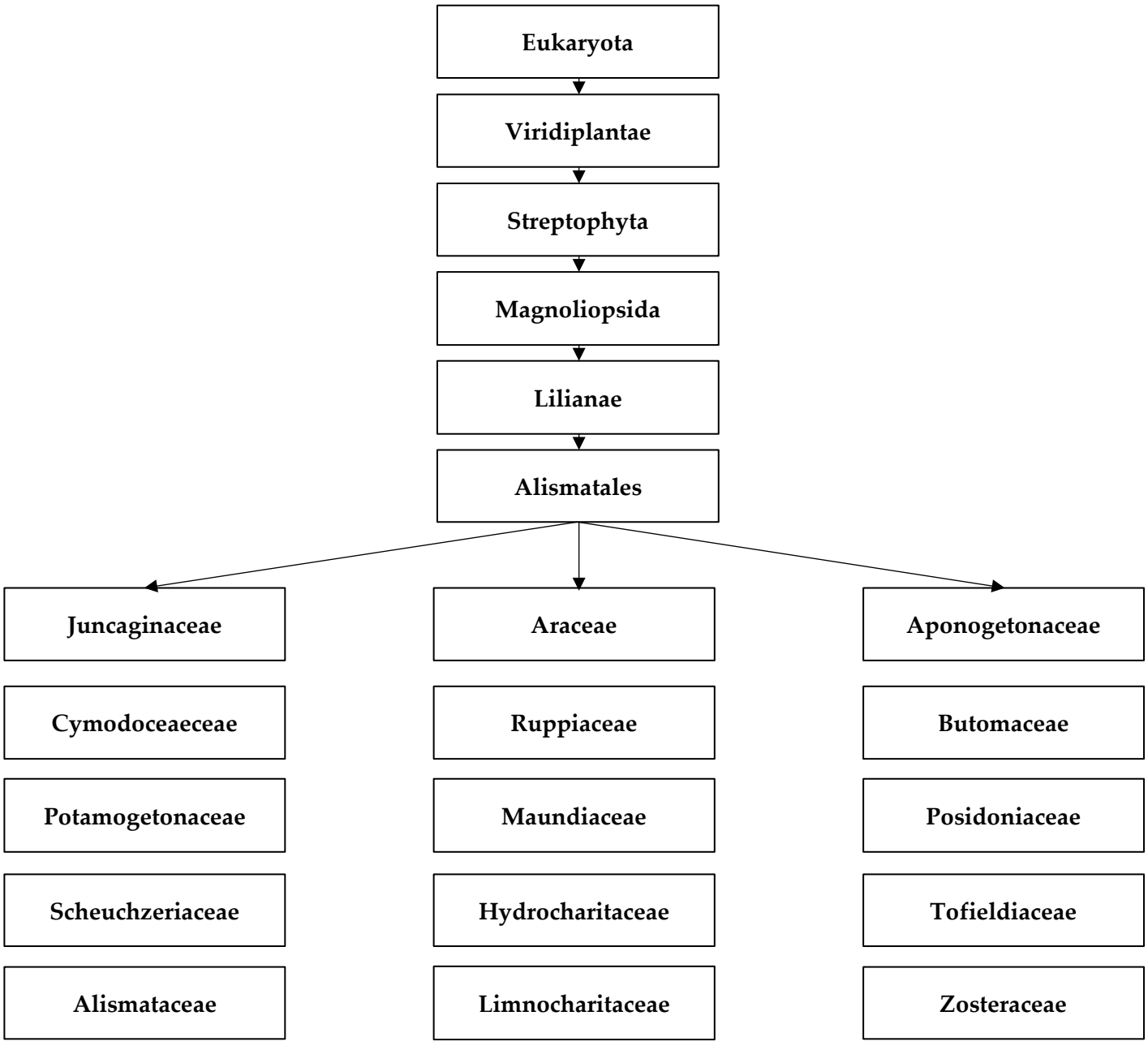

Figure: Taxononmy of Order Alismatales (Ruggiero, Gordon, 2014) (National Plant Data Center, MRCS, USDA, 1996). Only four familes of higher plants (Posidoniaceae, Cymodoceaceae, Hydrocharitaceae, Zosteraceae) contain exclusively marine species.

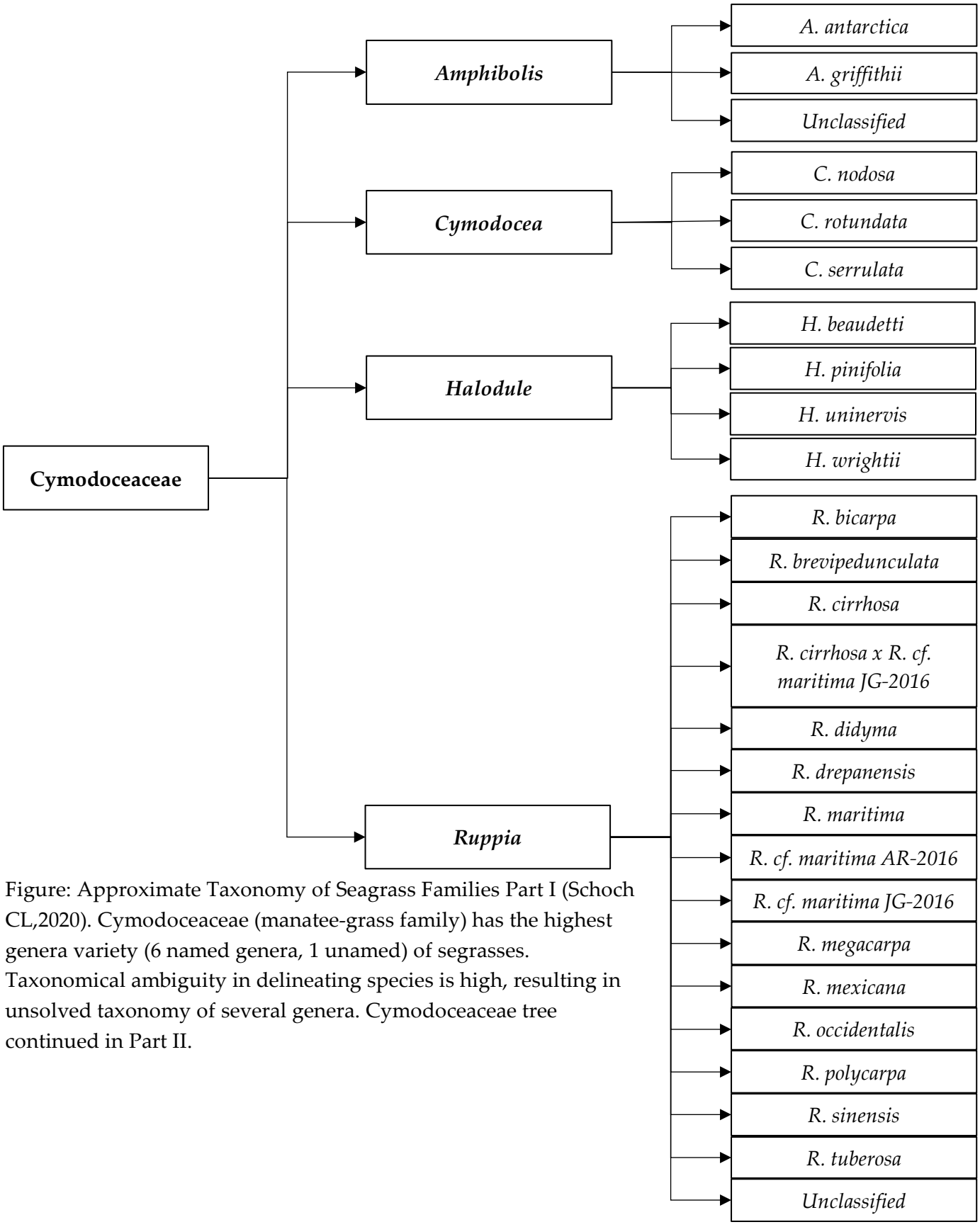

Figure: Approximate Taxonomy of Seagrass Families Part I (Schoch CL,2020). Cymodoceaceae (manatee-grass family) has the highest genera variety (6 named genera, 1 unamed) of segrasses. Taxonomical ambiguity in delineating species is high, resulting in unsolved taxonomy of several genera. Cymodoceaceae tree continued in Part II.

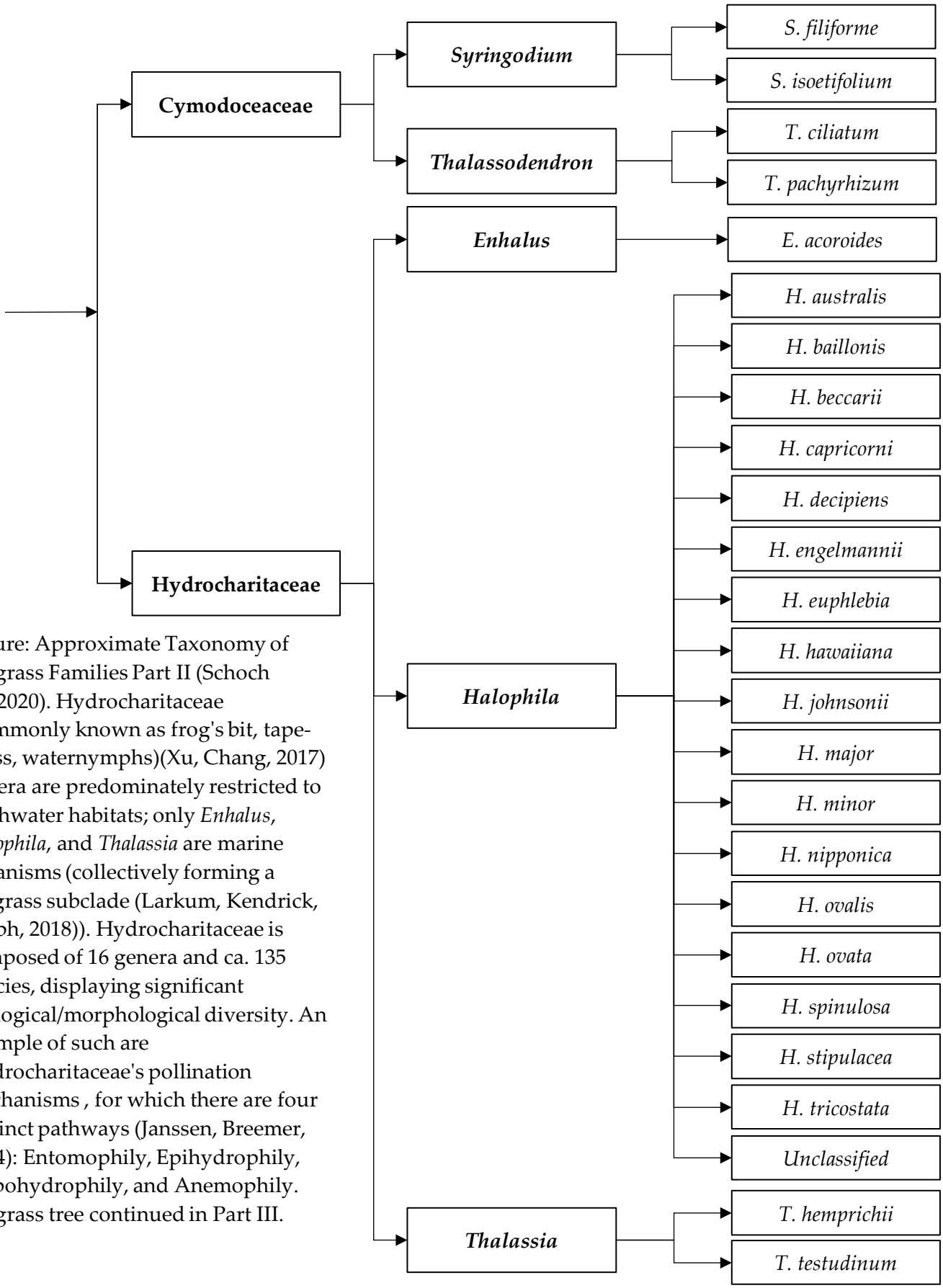

Figure: Approximate Taxonomy of Seagrass Families Part II (Schoch CL,2020). Hydrocharitaceae (commonly known as frog's bit, tape-grass, waternymphs)(Xu, Chang, 2017) genera are predominately restricted to freshwater habitats; only *Enhalus*, *Halophila*, and *Thalassia* are marine organisms (collectively forming a seagrass subclade (Larkum, Kendrick, Ralph, 2018)). Hydrocharitaceae is composed of 16 genera and ca. 135 species, displaying significant ecological/morphological diversity. An example of such are Hydrocharitaceae's pollination mechanisms , for which there are four distinct pathways (Janssen, Breemer, 2004): Entomophily, Epihydrophily, Hypohydrophily, and Anemophily. Seagrass tree continued in Part III.

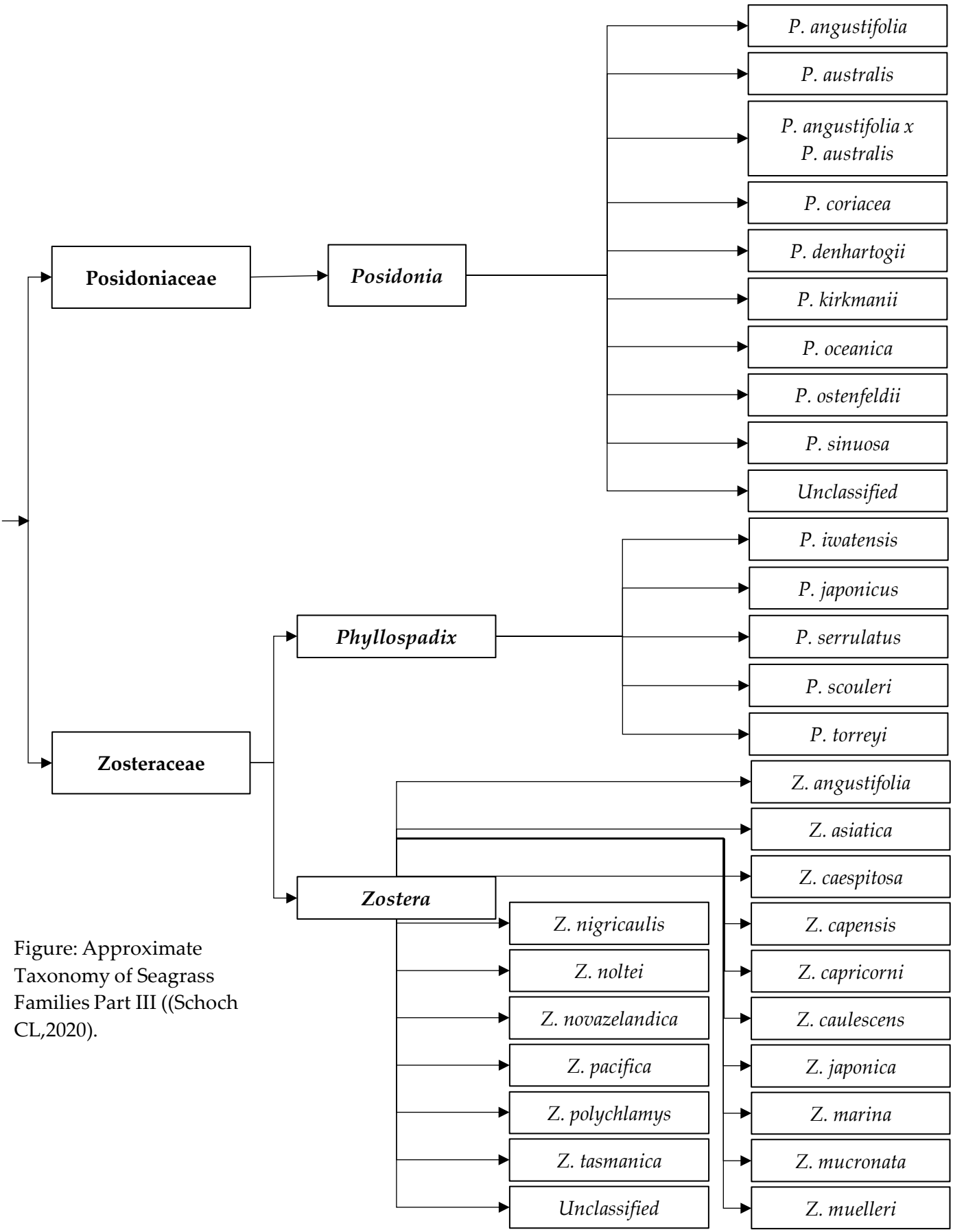

Figure: Approximate Taxonomy of Seagrass Families Part III ((Schoch CL,2020).

Background

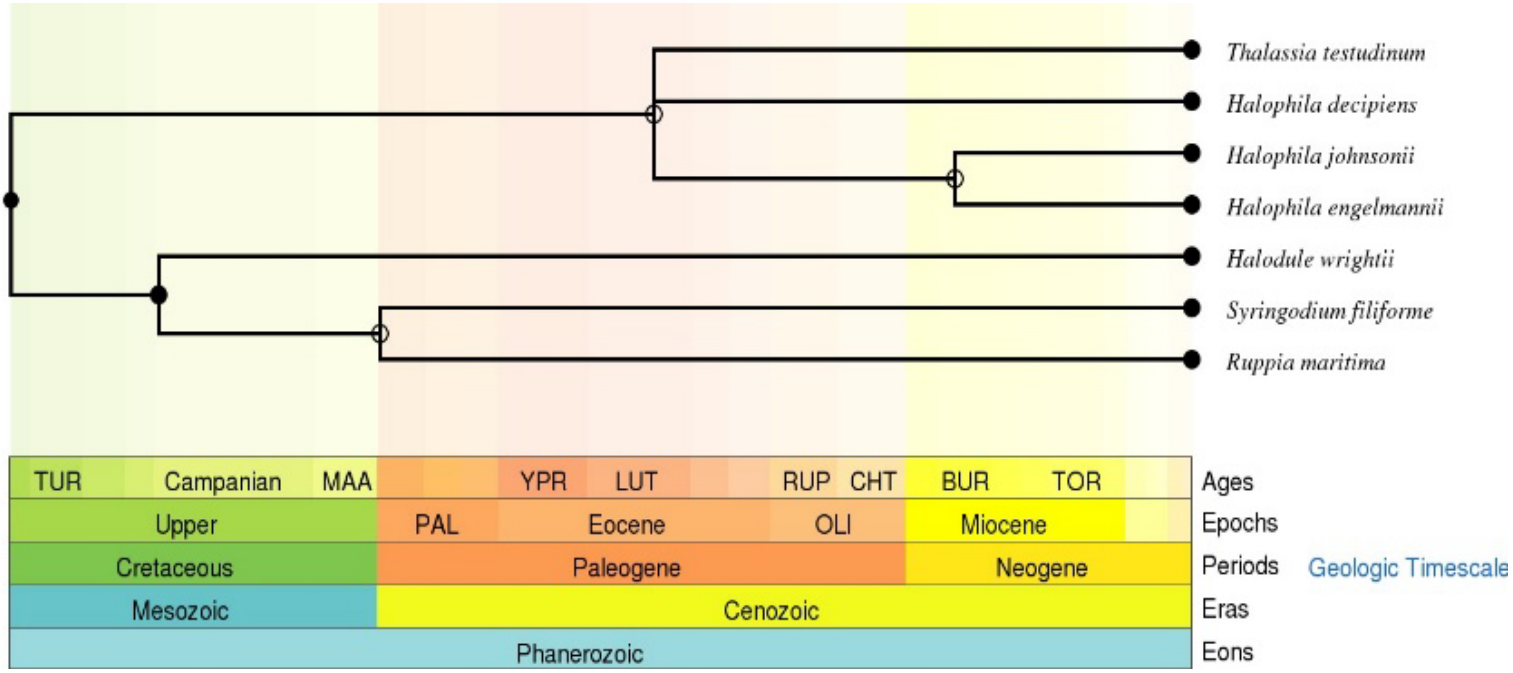

Figure: Timetree and divergence time of IRL indigenous seagrasses, generated with TimeTree (Kumar, Stecher, Suleki, Hedges, 2017).

Seagrasses can be classified as a paraphyletic group of marine angiosperm monocots that evolved from terrestrial plants (Larkum, Kendrick, Ralph, 2018), united biologically by their ability to grow in completely submerged marine environments. Among higher plants, whose ancestors left the sea some 400 MYA (Lee, Golicz, Bayer, Severn-Ellis, Chan, Batley, Kendrick, Edwards, 2018) seagrasses are the only group to completely return to the sea (Waycott, Biffin, Les, 2018), evolving independently at least four times over their evolutionary hisotry (Waycott, Biffin, Les, 2018). The phylogenetic history of marine monocotyledons is estimated to date into the mid-Cretaceous period (roughly 105 MYA) (Larkum, Kendrick, Ralph, 2018), leading way for two significant lineages to arise henceforth. These two groups retain elements of their more current counterparts.

Modern seagrasses vary with age and are considerably younger, starting to diverge about 70 million years ago (supported by fossil record and molecular clocking. The fossil record estimates Cymodoceaceae establishment in its Indo-West Pacific distribution by the early Eocene/late Paleocene (Brasier M.D, 1975), and fossils of Thalassodendron auriculalopris and Cymodocea floridana (found in west-central Florida) date back to the late middle Eocene (Lumbert, Hartog, Philips, Olsen, 1984). Their estimated age (crown node age of 61 MYA, stem node age of 67 MYA) (Janssen, Bremer, 2004) and lack of diversity suggests an extremely slow rate of evolution (Larkum, Hartog, 1989). The Hydrocharitaceae have a crown node age of 75 MYA and a stem node age of 88 MYA (Larkum, Kendrick, Ralph, 2018), Posidoniaceae only a stem node of 67 MYA can be estimated. Zosteraceae appeared the most recently, with a crown age of 17 MYA and a stem node age of 47 MYA.

While not touched upon in this investigation, it is noteworthy to mention persuing phylogeography (incorporating phylogenetic information into theory explaining geographic distribution of species) in the future is wise; it is important to preserve and document genetic material of remaining seagrasses. Promoting genetic diversity within re-establishment populations will be key in their long term recovery.

Background

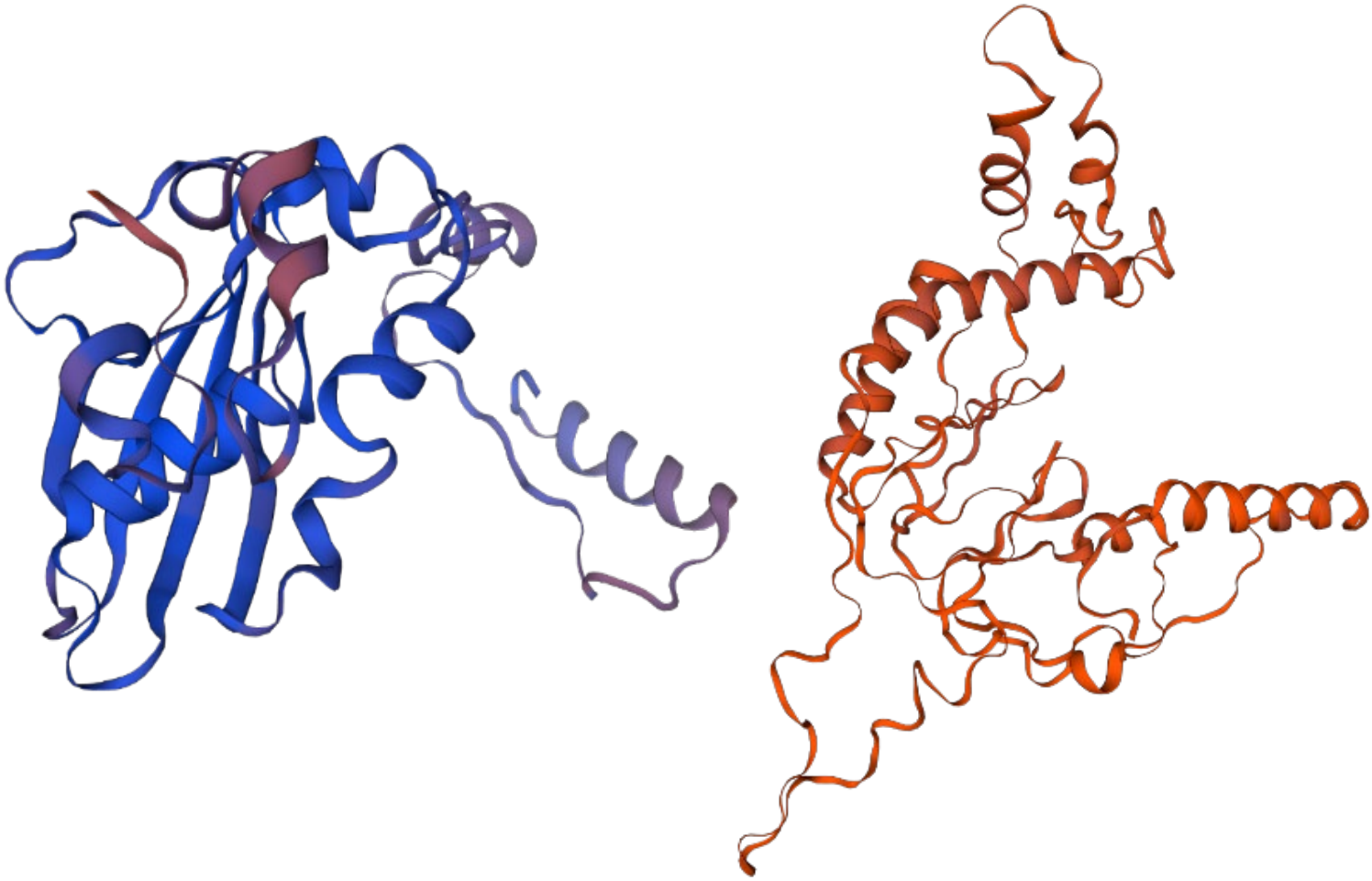

Phylogenetic relationships and divergence time estimates were calculated using two chloroplast DNA gene regions, *rcbL* and *matK* (pictured top left and right, respectively, generated using the SWISS-MODEL) (see works cited for full citation). By integrating molecular data into cladistic analysis methods, phylogenetic reconstructions of seagrass relationships can be further refined. DNA barcoding is such a method: species-level identification is achieved through use of DNA sequences from a signature region of the genome (Hebert et al., 2003). The Consortium for the Barcode of Life (CBOL) Plant Working group reccommends using plastid DNA (ptDNA) genes ribulose bisphosphate carboxylase large chain (*rbcL*) and maturase K (*matK*) as standard DNA barcode markers (CBOL Plant Working Group, 2009).

Of plastid regions, *rcbL* is the best characterized gene; the availability of universal primers has made it easily retrievable, and is well suited for recovery of high-quality bidirectional sequences [bidirectional promotors refer to the intergenic region between two adjacent genes transcribed in the opposite direction; good design can drive the expression of two genes simultaneously, and is critical for transgenic breeding for functionally related genes to express in the same pattern in the receptors (Vogl, Kickenweiz, Pitzer, 2018)]. *matK* is a leading barcode locus, and has been suggested as a universal barcode locus in land plants (CBOL Plant Working Group, 2009), consistently showing high levels of discrimination within angiosperm species. Historically, amplification and sequencing of the *matK* barcoding region has been challenging due to high sequence variability in primer binding sites (Hollingsworth, Graham, Little, 2011); within in the last decade this has been alleviated and methods for efficient PCR amplification/sequencing of *matK* are available (Heckenhauer, Barfuss, Samuel, 2016).

Background

In a previous study, tree- and character-based approaches were performed: *rbcL* sequence fragments were shown to resolve up to family and genus level, *matK* sequences resolving species-level and partial ecotype-level (Lucas, Thangaradjou, Papenbrock, 2012). The focus of their work was to develop a DNA barcoding system to help with the identification of regional seagrasses, with the scope of the work keyed into 14 seagrass species found in India (supplemented by other temperate seagrass data). The bioinformatic analysis presented here is based off their work.

The *rcbL* and *matK* sequence data was retrieved from the NCBI Nucleotide Database and aligned using both MUSCLE and Clustal Omega (see works cited for full citations).

Alignment	*matK*
Sequences Utilized	KF488511.1 Syringodium filiforme voucher C2611 maturase K (matK) gene, partial cds; plastid JN225379.1 Halodule wrightii from India maturase K (matK) gene, partial cds; chloroplast JX438642.1 Ruppia maritima maturase K (matK) gene, partial cds; chloroplast JX457605.1 Halophila decipiens voucher HO2011015 maturase K gene, partial cds; chloroplast

Alignment	*rbcL*
Sequences Utilized	U03727.1 Syringodium filiforme chloroplast ribulose-1,5-bisphosphate carboxylase/oxygenase large subunit (rbcL) gene, partial cds HQ901575.1 Halodule wrightii ribulose-1,5-bisphosphate carboxylase/oxygenase large subunit (rbcL) gene, partial cds; plastid HQ901568.1 Thalassia testudinum ribulose-1,5-bisphosphate carboxylase/oxygenase large subunit (rbcL) gene, partial cds; plastid HQ901576.1 Ruppia maritima ribulose-1,5-bisphosphate carboxylase/oxygenase large subunit (rbcL) gene, partial cds; plastid U80698.1 Halophila decipiens ribulose-1,5-bisphosphate carboxylase/oxygenase large subunit (rbcL) gene, chloroplast gene encoding chloroplast protein, partial cds

The analysis broke into two paths: one set of phylogenetic testing (MUSCLE aligned sequences) was loaded into MEGA-X, and the other (Clustal Omega aligned sequences) was loaded into BEAUti (see works cited for full citation), which is a graphical user-interface application for generating BEAST XML files.

Background

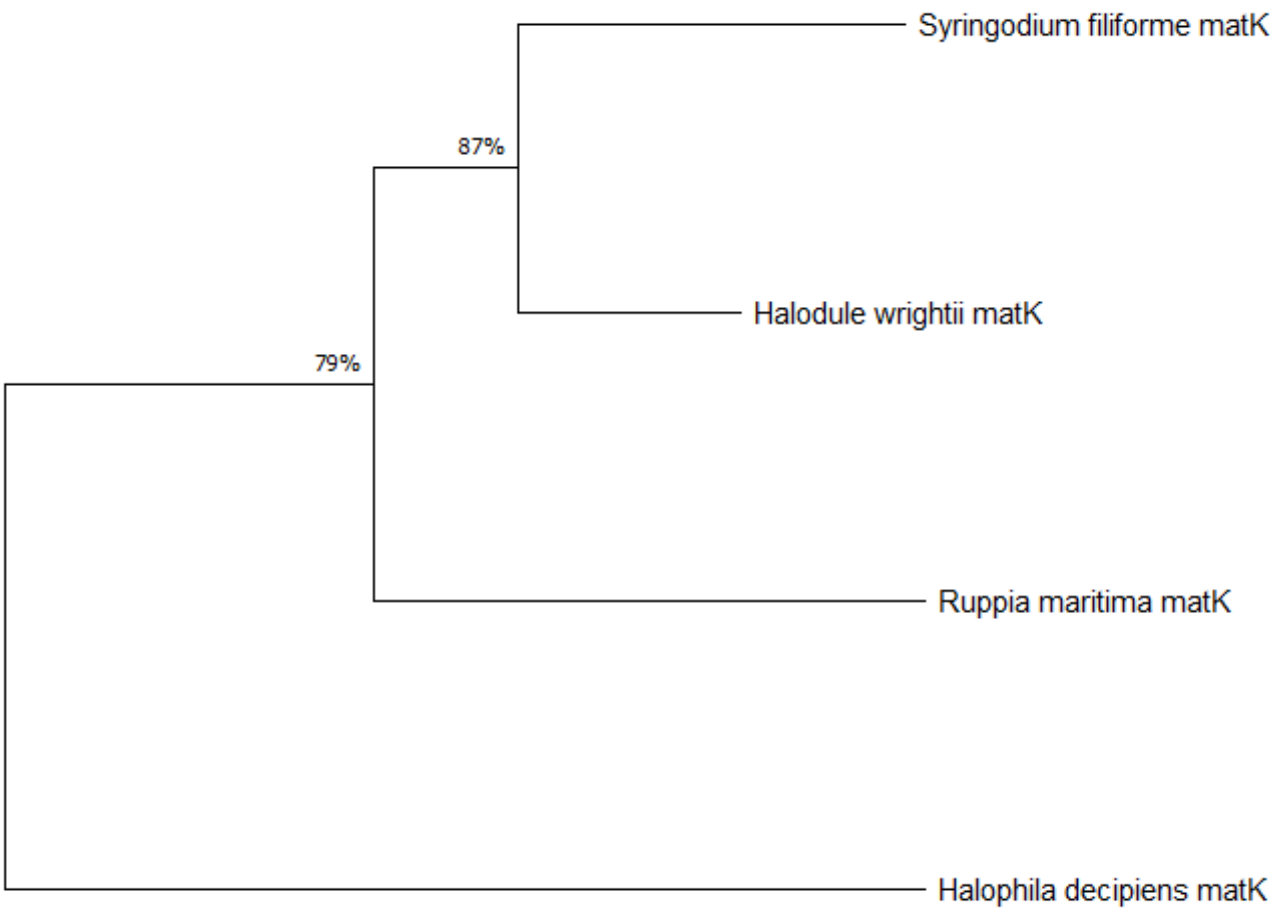

Figure: Evolutionary analysis by Maximum Likelihood method (MUSCLE-aligned)
The evolutionary history was inferred by using the Maximum Likelihood method and General Time Reversible model [1]. The tree with the highest log likelihood (-2246.13) is shown. The percentage of trees in which the associated taxa clustered together is shown next to the branches. Initial tree(s) for the heuristic search were obtained automatically by applying Neighbor-Join and BioNJ algorithms to a matrix of pairwise distances estimated using the Maximum Composite Likelihood (MCL) approach, and then selecting the topology with superior log likelihood value. The tree is drawn to scale, with branch lengths measured in the number of substitutions per site. The proportion of sites where at least 1 unambiguous base is present in at least 1 sequence for each descendent clade is shown next to each internal node in the tree. This analysis involved 4 nucleotide sequences. Codon positions included were 1st+2nd+3rd+Noncoding. There were a total of 928 positions in the final dataset. Evolutionary analyses were conducted in MEGA X [2]

1. Nei M. and Kumar S. (2000). Molecular Evolution and Phylogenetics. Oxford University Press, New York.
2. Kumar S., Stecher G., Li M., Knyaz C., and Tamura K. (2018). MEGA X: Molecular Evolutionary Genetics Analysis across computing platforms. Molecular Biology and Evolution 35:1547-1549.
3. Felsenstein J. (1985). Confidence limits on phylogenies: An approach using the bootstrap. Evolution 39:783-791.

Background

[Analysis Settings]

Statistical Method = Maximum Likelihood
Test of Phylogeny = Bootstrap method
No. of Bootstrap Replications = 10000
Substitutions Type = Nucleotide
Model/Method = General Time Reversible model
Rates among Sites = Uniform Rates
Gaps/Missing Data Treatment = Use all sites
Select Codon Positions = 1st,2nd,3rd,Non-Coding
Initial Tree for ML = Make initial tree automatically (Default = NJ/BioNJ)
Branch Swap Filter = None
Number of Threads = 7

Num of params = 13
Num of rates = 1
AICc = 4518.370
BIC = 4597.896
LnL = -2246.131
Invar = n/a
Gamma = n/a
Ts/Tv = 1.135
r(A->T) = 0.0172369012400884
r(A->C) = 0.0835716843804826
r(A->G) = 0.076370873003538
r(T->A) = 0.0133223892249283
r(T->C) = 0.0859644608493788
r(T->G) = 0.0373346157957188
r(C->A) = 0.154857876138789
r(C->T) = 0.206096284540888
r(C->G) = 0.029962027666278
r(G->A) = 0.160112240937602
r(G->T) = 0.10127110362658
r(G->C) = 0.0338995425957273

Discussion:

Maximum Likelihood (ML) is a statistical inference framework used for estimating parameters in a probabilistic data generating model (Dhar, Minin, 2016). The approach generates the probabilities of sequences given a model of their evolution on a particular tree; when provided sequence parameters, the tree with the highest likelihood score is optimal (Singh, Pathak, 2021). The model of evolution (General Time Reversible model, GTK) is the model of nucleotide substitution; six possible substitution types exist among the four nucleotides, resulting in 203 possible transformation matrices (base frequency may be assumed to be equal or variable) (Sullivan, Joyce, 2005). Tree construction and branch length calculations are performed by using evolutionary probabilities of nodal connections (probabilities are based off a stochastic model of sequence evolution (Brahme, 2014)). Alternative tree topologies are readily evaluated using associated likelihoods, i.e evaluating the effect of including one or more parameters by calulating a likelihood model where the parameter of interest is optimized via model comparison. It should be mentioned that likelihood methods are difficult to be applied to large data sets and can fall into local traps (Golding, Felsenstein, 1990).

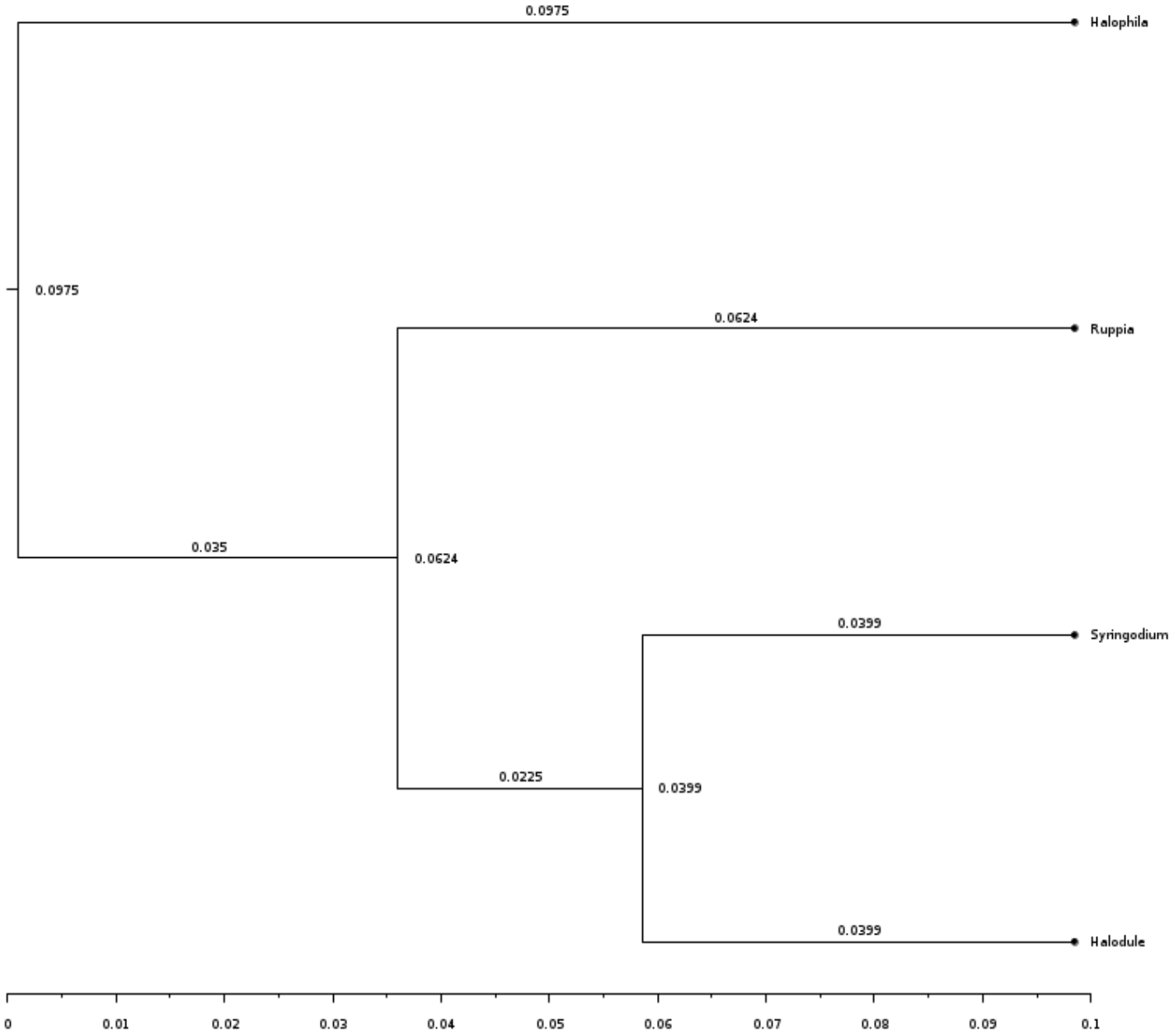

Figure: Tree generated with the use of Clustal Omega, BEAUti 2, BEAST 2, and FigTree v1.4.4. Node ages are labeled at nodes and branch times labled on branches. BEAST (Bayesian Evolutionary Analysis Sampling Trees) is a package for evolutionary inference from molecular sequences, and widely used within the bioinformatic community. It estimates rooted, time-measured phylogenies using strict or relaxed molecular clock models, and can be used as a method for reconstructing phylogenies and for testing evolutionary hypothesis without conditioning on a single tree topology. BEAST 2 uses Markov chain Monte Carlo (MCMC) to average over tree space, so that each tree is weighted proportional to its posterior probability. In order to create this tree, the *matK* sequence list was aligned using Clustal Omega using default settings (output file type .fasta), then imported into BEAUti 2 (Bayesian Evolutionary Analysis Utility), a graphical user-interface (GUI) application for creating BEAST XML files. From there, BEAST 2 was initiated, generated 100001 trees, wrote them to file (.trees filetype), and that file loaded into FigTree (where tree 100001 was labeled and exported as a PDF).

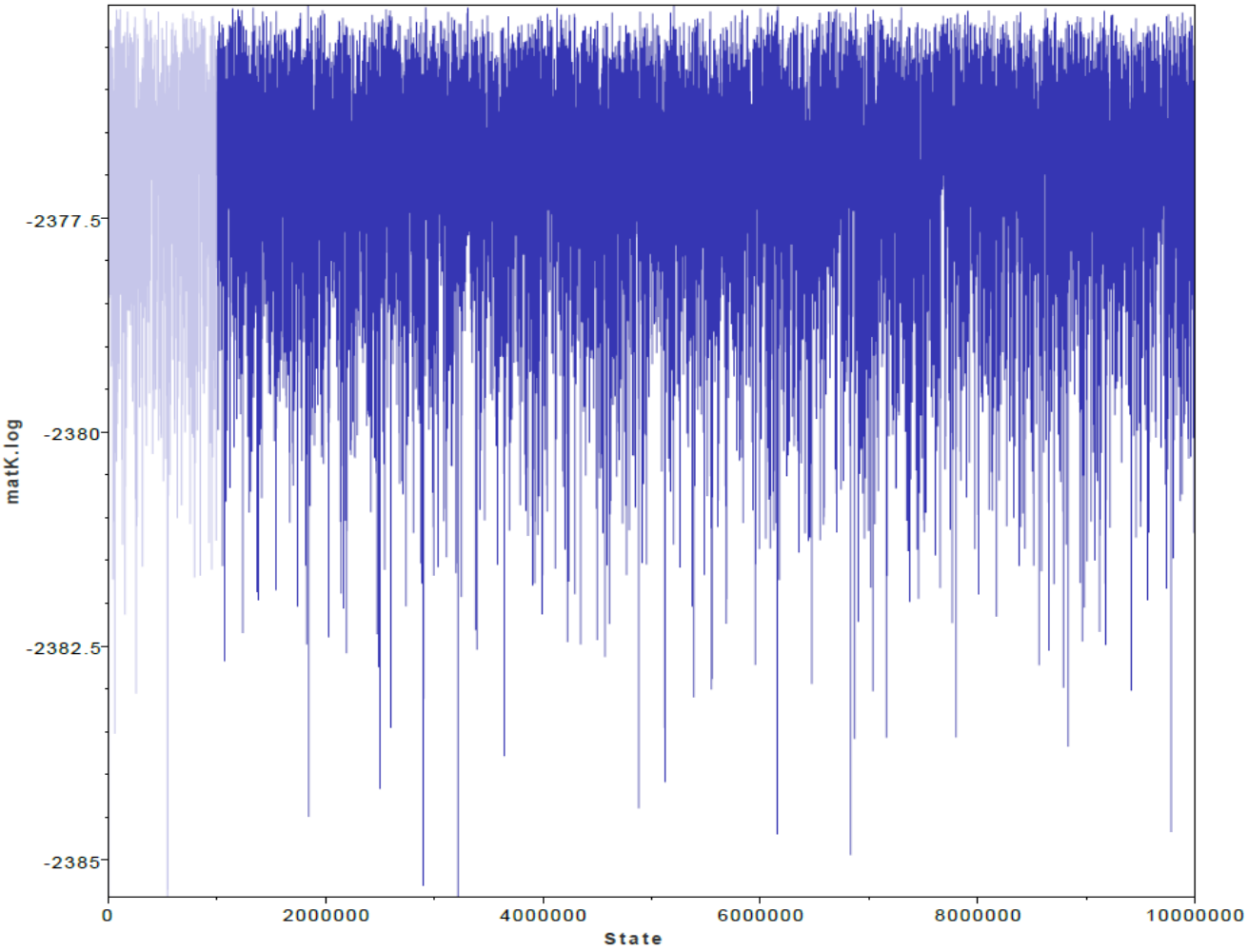

Figure: Raw *matK* trace (generated with Tracer1.7.2) (Rambaut, Drummond, Xie, Baele, Suchard, 2018), visualizing posterior probability change as MCMC proceeds.

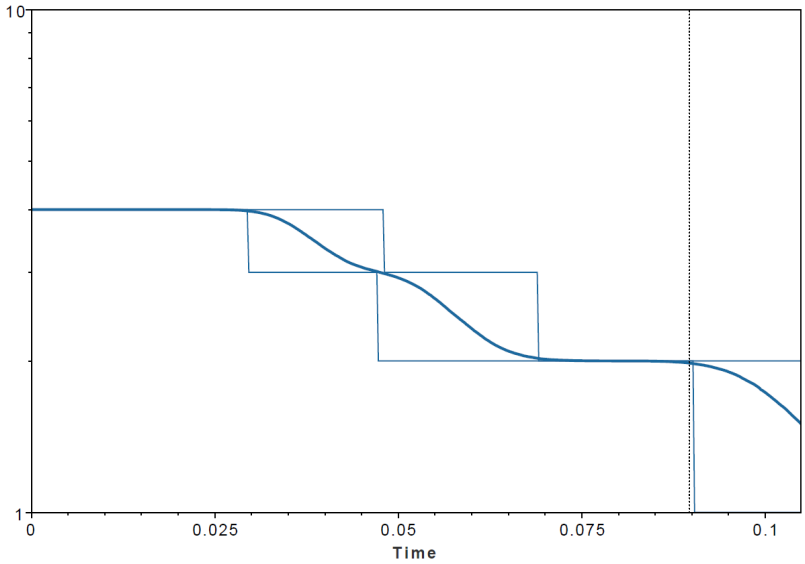

Figure: Lineage-through-time (LTT) plot from posterior distribution of sampled tree topologies using Tracer1.7.2 (Rambaut, Drummond, Xie, Baele, Suchard, 2018)

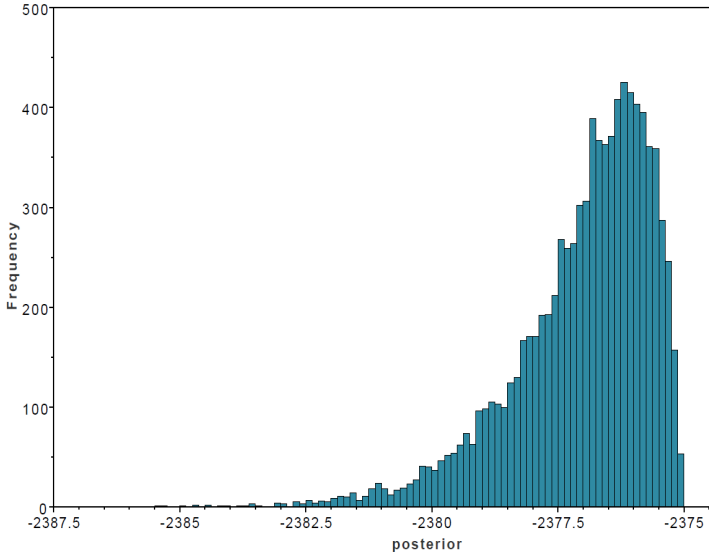

Figure: Frequency of posterior probabilities, generated with Tracer1.7.2 (Rambaut, Drummond, Xie, Baele, Suchard, 2018)

Background

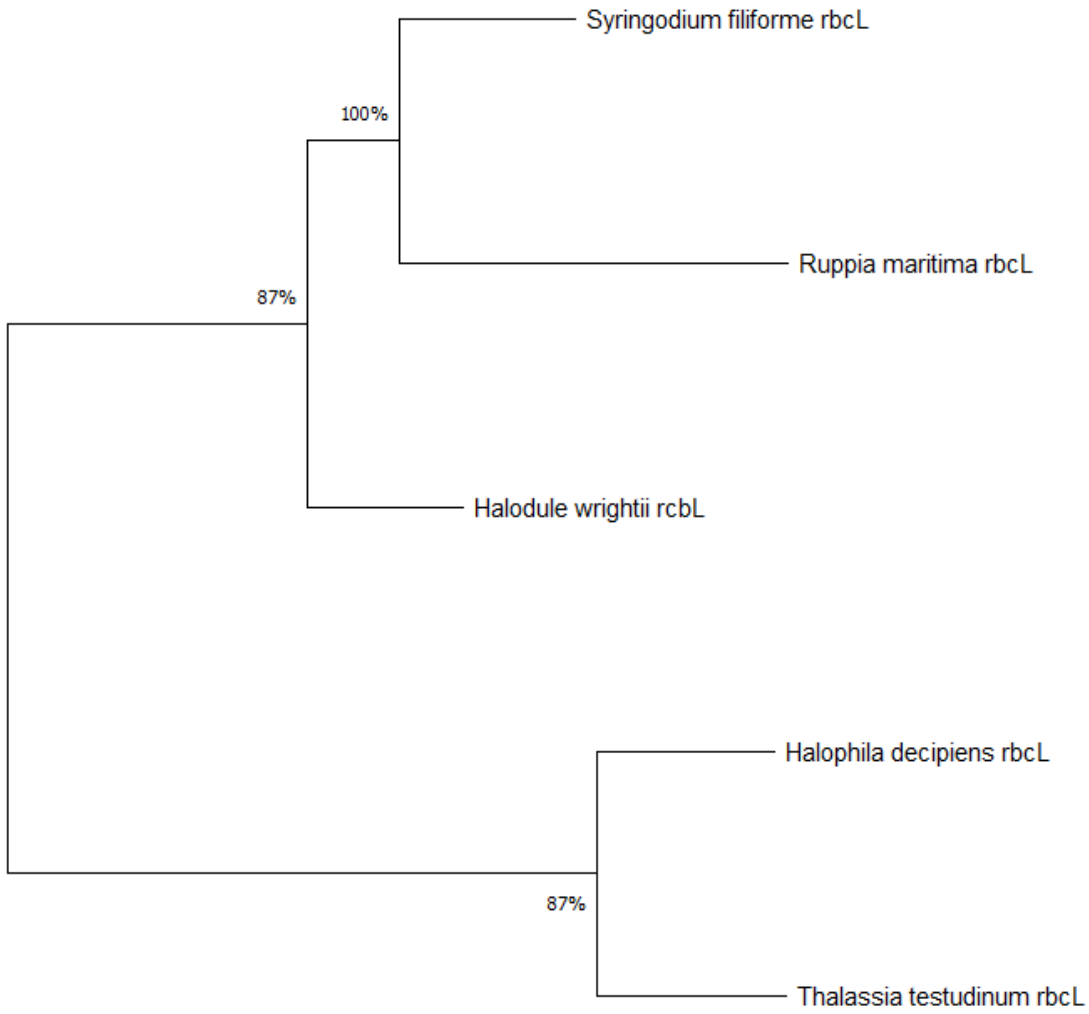

Figure: Evolutionary analysis by Maximum Likelihood method (MUSCLE-aligned)
The evolutionary history was inferred by using the Maximum Likelihood method and General Time Reversible model [1]. The tree with the highest log likelihood (-2874.24) is shown. The percentage of trees in which the associated taxa clustered together is shown next to the branches. Initial tree(s) for the heuristic search were obtained automatically by applying Neighbor-Join and BioNJ algorithms to a matrix of pairwise distances estimated using the Maximum Composite Likelihood (MCL) approach, and then selecting the topology with superior log likelihood value. The tree is drawn to scale, with branch lengths measured in the number of substitutions per site. The proportion of sites where at least 1 unambiguous base is present in at least 1 sequence for each descendent clade is shown next to each internal node in the tree. This analysis involved 5 nucleotide sequences. Codon positions included were 1st+2nd+3rd+Noncoding. There were a total of 1348 positions in the final dataset. Evolutionary analyses were conducted in MEGA X [2]

1. Nei M. and Kumar S. (**2000**). *Molecular Evolution and Phylogenetics*. Oxford University Press, New York.
2. Kumar S., Stecher G., Li M., Knyaz C., and Tamura K. (**2018**). MEGA X: Molecular Evolutionary Genetics Analysis across computing platforms. *Molecular Biology and Evolution* **35**:1547-1549.
3. Felsenstein J. (1985). Confidence limits on phylogenies: An approach using the bootstrap. Evolution 39:783-791.

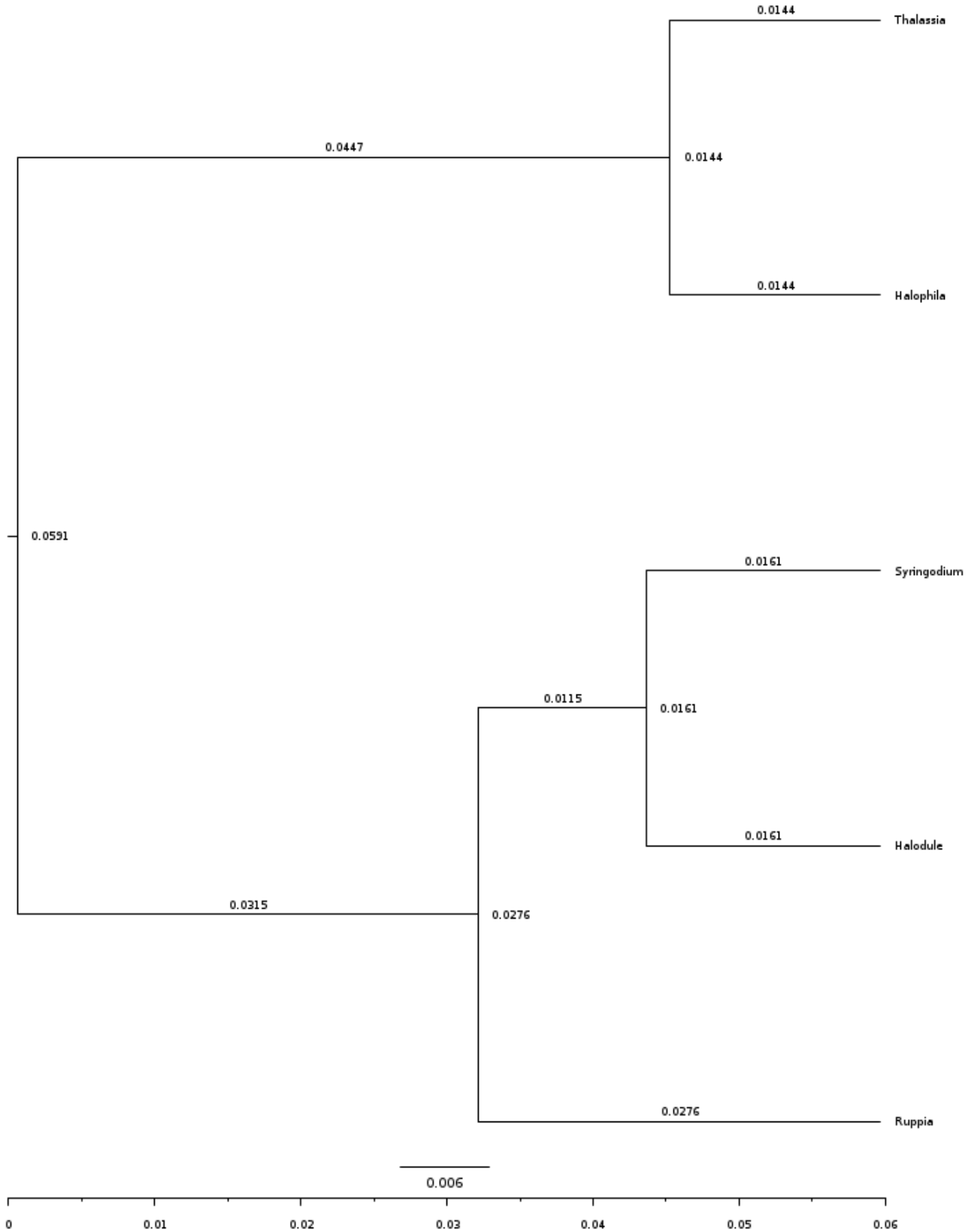

Figure: Figure: *rbcL* tree generated with the use of Clustal Omega, BEAUti 2, BEAST 2, and FigTree v1.4.4. Node ages are labeled at nodes and branch times labled on branches.

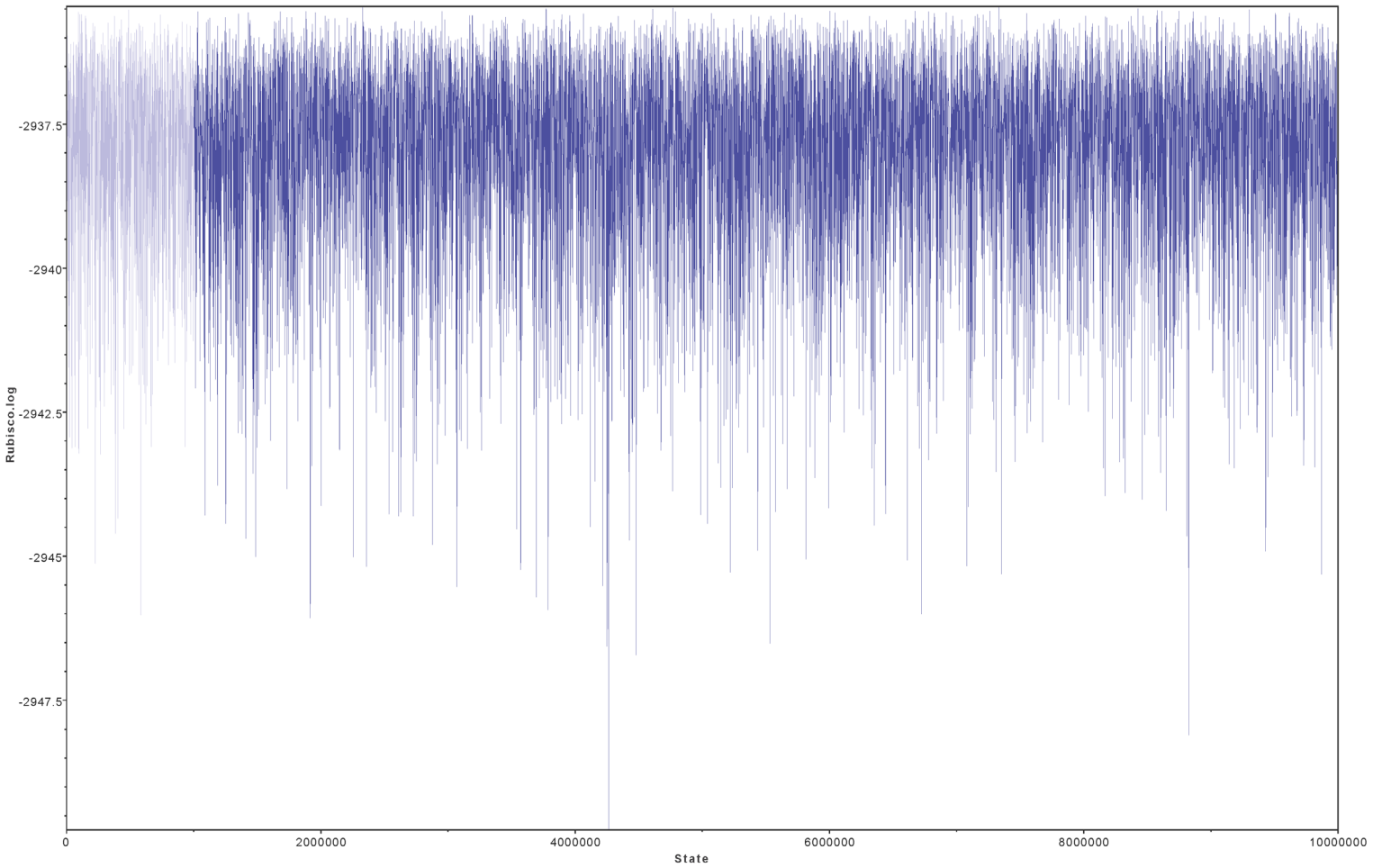

Figure: Raw *rbcL* trace (generated with Tracer1.7.2) (Rambaut, Drummond, Xie, Baele, Suchard, 2018), visualizing posterior probability change as MCMC proceeds.

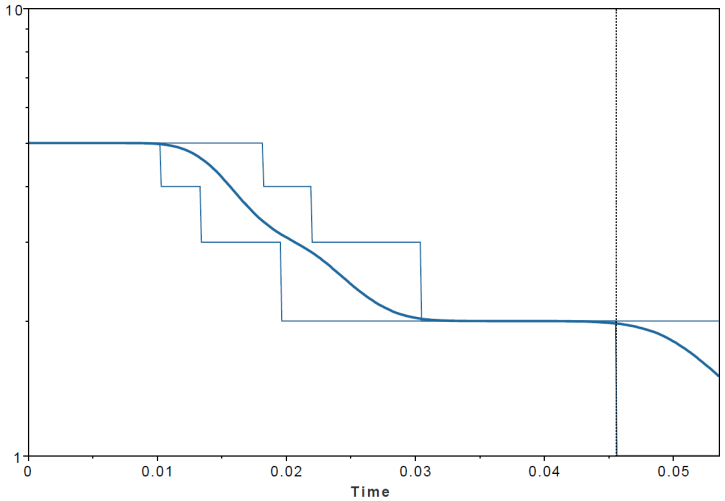

Figure: Lineage-through-time (LTT) plot constucted from posterior distribution of sampled tree topologies using Tracer1.7.2 (Rambaut, Drummond, Xie, Baele, Suchard, 2018)

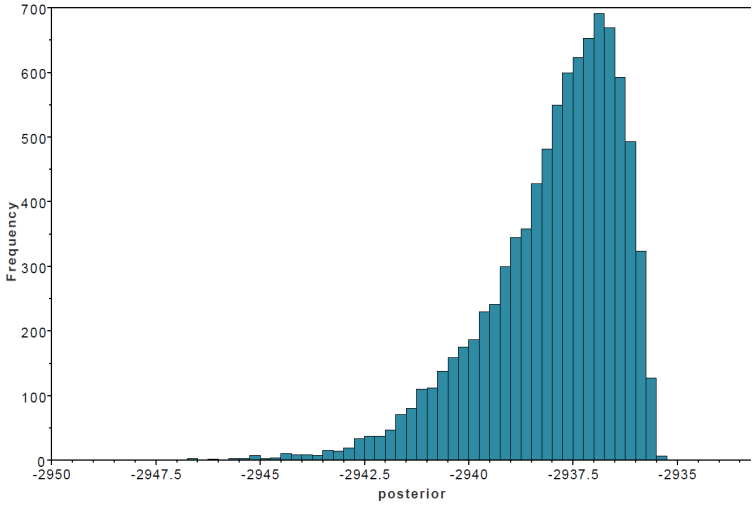

Figure: Frequency of posterior probabilities, generated with Tracer1.7.2 (Rambaut, Drummond, Xie, Baele, Suchard, 2018).

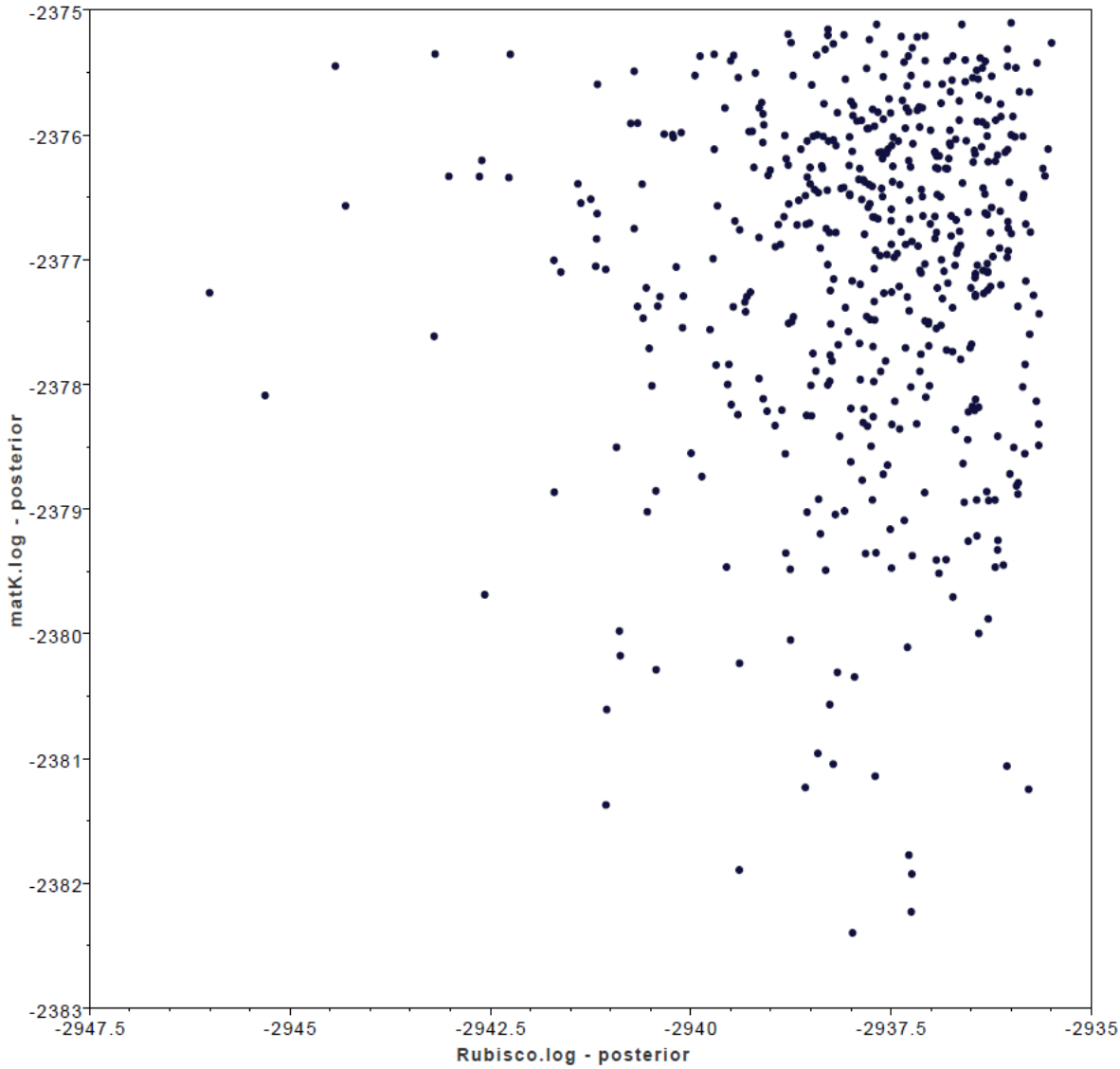

Figure: Scatter plot of two continuous parameters (posterior probability *rbcL* vs posterior probability *matK*) generated with Tracer1.7.2 (Rambaut, Drummond, Xie, Baele, Suchard, 2018), with the intent of identifying correlation between parameters.

Discussion of results:

While the purpose of this investigation is the development of a real time data acquisition/control system, it would not be prudent to omit the genetic aspect of seagrasses. A common assumption within conservation genetics is higher levels of genetic diversity within a population leads to an increase in fitness and long-term survival of a species. Promoting diversity within lab grown seagrasses is of extreme importance; if it is to be used as transplant material in the future, higher genetic diversity should contribute to hardiness of species and promote further diversification within existing populations (in turn strengthening them). Visualization of such requires knowledge of sequencing techniques and phylogenetics. The models provided here only begin to showcase the potential of modern systematic biological methods. Mathematical considerations (dictated by the nature of alignment(s)) must be given when designating test conditions in BEAUti2 for publication-level model generation: without knowledgeable justifications for testing parameters, it is unwise to make significant inferences. It is promising that trees drawn using two separate methodologies generated near-identical models; if errors exist, it's likely they are uniform throughout both datasets. Another point of interest is that according to the Lineage-through-time models, *rbcL* began significant evolution before *matK*, which when considering adaptations to photosynthesis required for marine life, could be argued as an implicit manifestation. The investigation looks forward to refining these methodologies in future works.

Background

Single-board computers offer a cost-effective means for develping customized embedded sytems in lieu of purchasing prefabricated advanced sensors and related software/interfaces. The Raspberry Pi Foundation (a UK-based charity), in association with Broadcom Inc, produce a series of small single-board computers (commonly referred to as Raspberry Pi, RPi, Raspi) that are popular educational/development devices given their modularity, open hardware platform, Linux compatibility, and active development community. This experimental design will utilize Raspberry Pi 3 Model B, which contains the following specifications:

SoC: Broadcom BCM2837
CPU: 4× ARM Cortex-A53, 1.2GHz
GPU: Broadcom VideoCore IV (3D part of GPU runs at 300 MHz, video part runs at 400MHz)
RAM: 1GB LPDDR2 (900 MHz) (shared with GPU)
Networking: 10/100 Ethernet, 2.4GHz 802.11n wireless
Bluetooth: Bluetooth 4.1 Classic, Bluetooth Low Energy
Storage: microSD
GPIO: 40-pin header, populated
Ports: HDMI, 3.5mm analogue audio-video jack, 4× USB 2.0, Ethernet, Camera Serial Interface (CSI), Display Serial Interface (DSI)
Power source: 5V via MicroUSB (can be powered through onboard GPIO additionally)
Power ratings: 800 mA (4W)

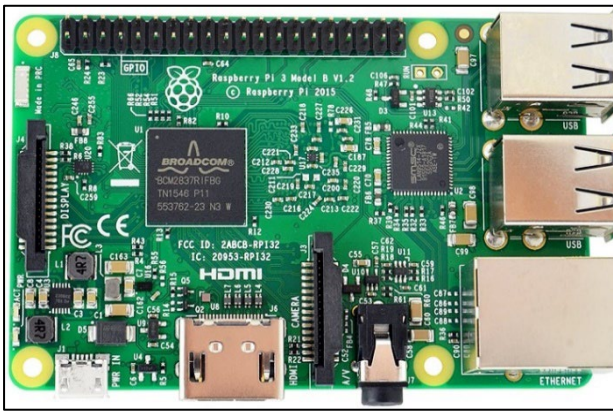

Figure 3: Raspberry Pi 3 Model B (Amazon, 2021). Released in Febuary 2016, it serves as a substantial upgrade to its predecessor, Pi 2.

The 40-pin general-purpose input-output (GPIO) port allows the Pi to act as a controller in larger electronic circuits; it will be seated in the Robo-Tank Aquarium Controller (running reef-pi) and will be capable of:

- **Equipment control** (real time/periodic timers)
- **Salinity control** (Auto Top Off controller)
- **Temperature control** (monitoring/heaters/coolers)
- **Light simulation** (diurnal, lunar cycle simulation)
- **pH control** (continuous monitoring, dosing)
- **Automated dosing** (calcium, alkalinity)
- **Macros** (automate multi-step processes, i.e. water change)
- **Telemetry** (dashboard, charts, text/email alerting)

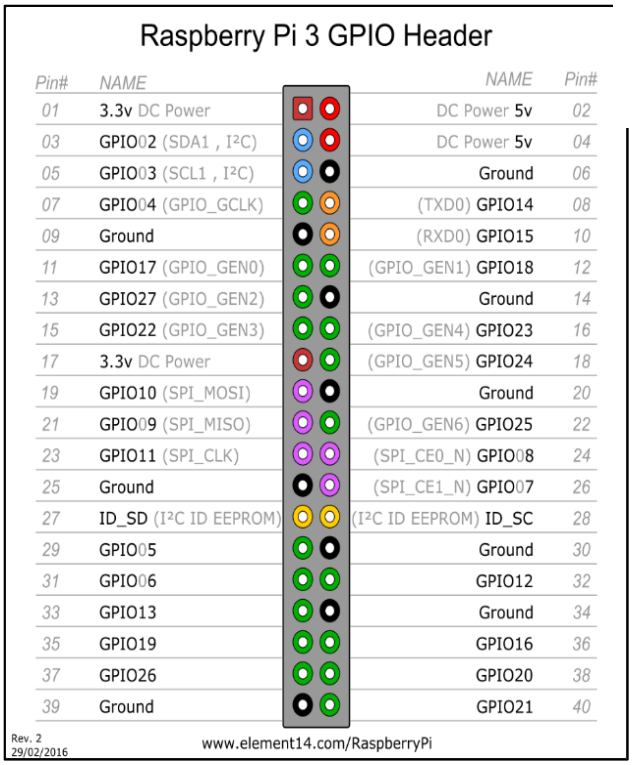

Figure 4: GPIO pin breakout for the Raspberry Pi 3 Model B (Chan, duMais, 2021)

For greater detail on Raspberry Pi, please refer to the technical insert provided.

Background

The controller software being utilized in the experimental design is reef-pi, an award-winning opensource reef aquarium controller project created/led by Ranjib Dey (in addition, Vincent le Goff and Michael Lane are co-maintainers), and has been featured in articles published by Make, Adafruit, and the Raspberry Pi Foundation. It is primarily written in React (JavaScript library for building user interfaces, frontend) and Go (runs web server, backend).

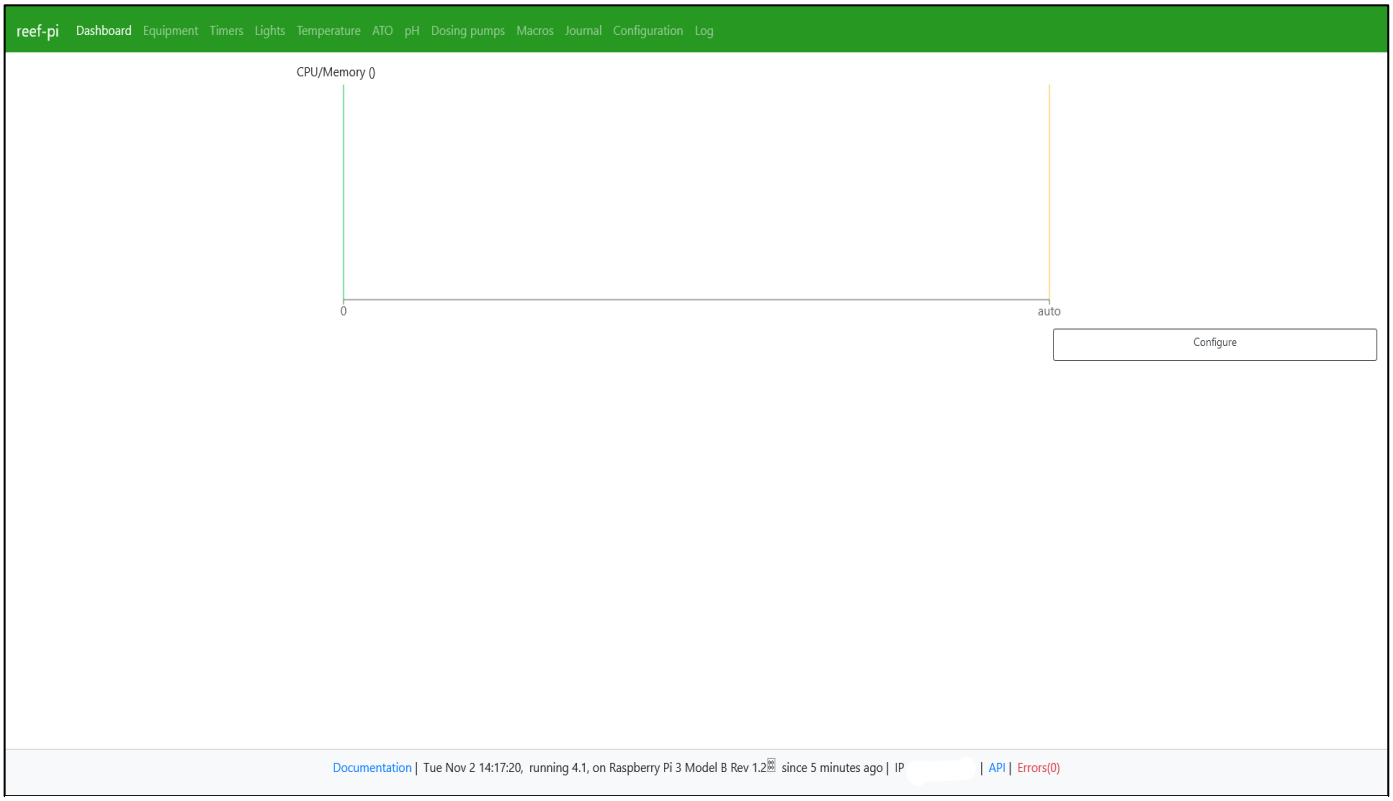

Figure 5: Current reef-pi Dashboard view, generated by the investigation's prototype construct. The user interface (UI) can be accessed by anyone on the same network (credentials provided), and it is possible to run in a "headless" (no monitor or keyboard connected) state.

Figure 6: Populated Dashboard (image from Ranjib Dey's Reef2Reef build thread)

Background

reef-pi is modular in nature (functionality is definied by Raspberry Pi, controller software, peripheral circuity) and highly adaptable (lending itself favorible for custom builds). Furthermore, the opensource community that surrounds the project is thriving; individuals detailing their builds/troubleshooting methods are numerous, overwhelmingly helpful, and eager to see the project improve. Preliminary designs for all periherial circuity were based off Ranjib Dey's designs outlined in his Adafruit Learning System Guides for reef-pi and various builds posted on the Reef2Reef Reef-Pi Discussion Forums.

While these designs are excellent prototypes (and operate well in practice), basing a research-grade embedded system on Perma-Proto Hats (which are used for development purposes and aren't permanent PCB's typically) is not prudent. Preferably the Pi should mate with an integrated circuit.

There is also the issue of monitoring conductivity, dissolved oxygen, and flow meters; these functionalities do not exist within reef-pi currently and needs to be addressed (most likely drivers will need to be written and added via the Application Programming Interface).

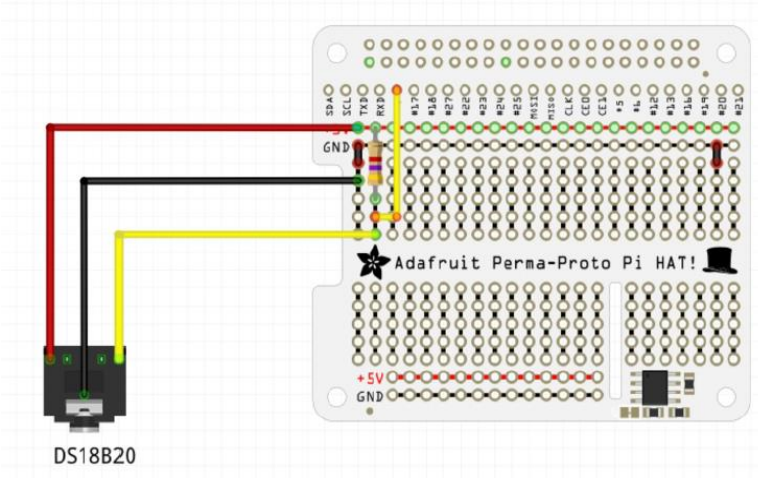

Figure 7: Temperature Sensor (Dey, 2019): Two of the male header pin are directly connected to GND and 3.3V while the 4.7K resistor is used as a pull-up resistor (from the 3.3V power) on the data pin (center). Though there is only a single DS18B20 sensor seen here, it should be possible to connect up to 7 sensors, since the wiring would be the same (underlying one-wire protocol is a bus going to GPIO4). It should be noted that DS18B20 are notorious for not being shielded properly, warrants further investigation.

Figure 8: Full Temperature Sensor Circuit (Dey,2019) including power controller circuit. The termperature controller module in reef-pi doesn't require power controller implementation (i.e. temperature monitoring/logging is the objective); however turning on/off heaters or chillers will require a functional power controller, which entails creating a power strip control ciruit using a ULN2803A Darlington transitor (converts Raspberry Pi GPIO 3.3V to 12V), a 12V power supply (for both Pi and power strip control circuit), and a LM2596 Buck Converter to convert 12V to 5V (so the Pi and the power strip can use a single power supply).

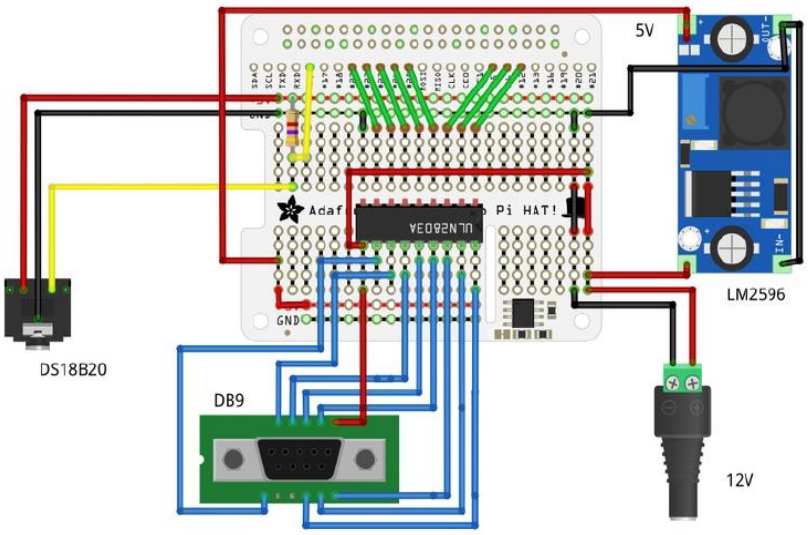

Background

Robo-Tank is a fully automated aquarium controller designed/maintained by Robert Fowler, and has both software and hardware components. While the software is still under development (not yet opensource; should be noted the investigation is actively monitoring/assisting with development), the hardware is fully functional, interfaces with the Raspberry Pi via GPIO, and can be utilized easily with reef-pi.

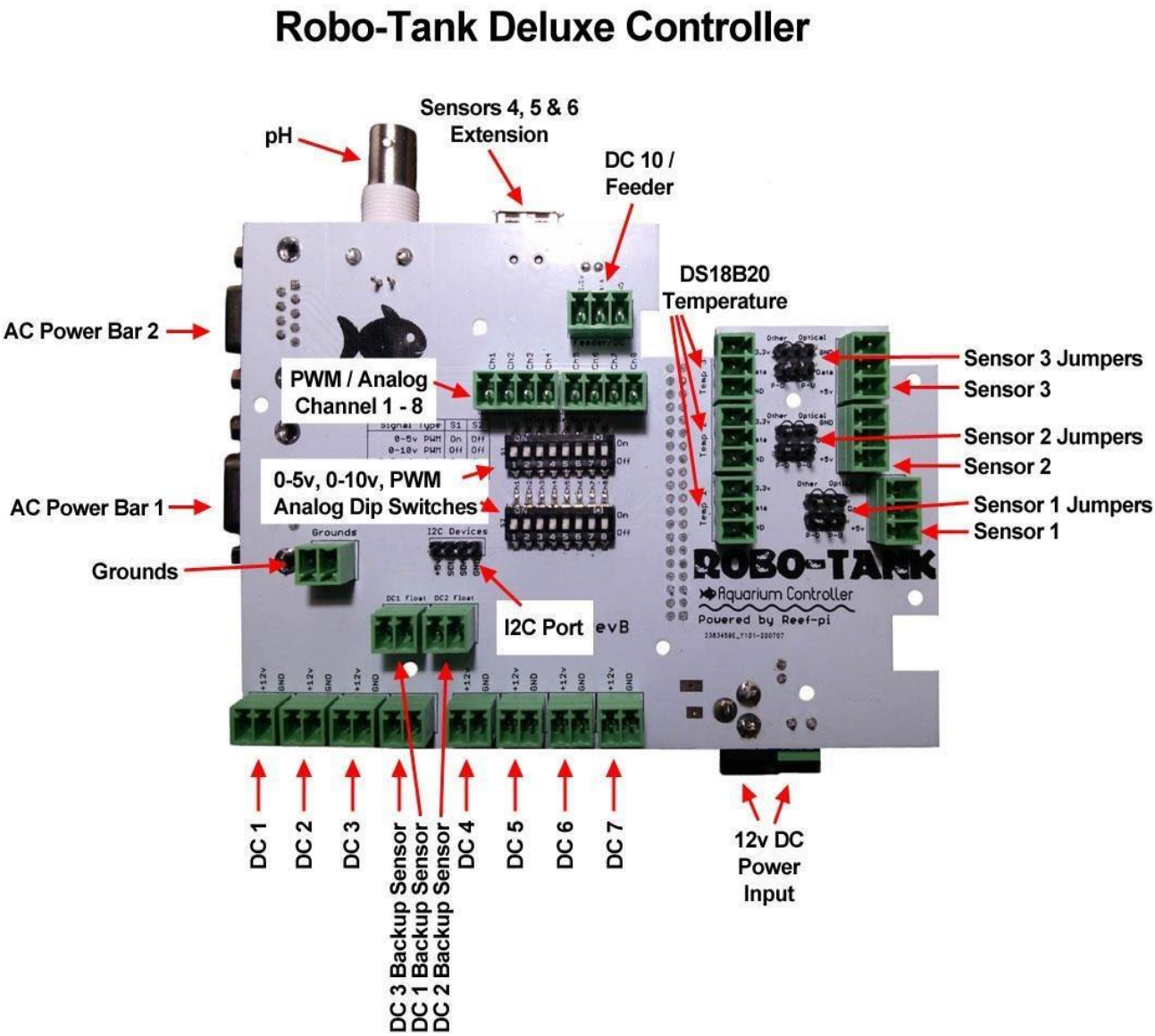

Figure 9: Robo-Tank Aquarium Controller Top View (Fowler, 2019). There are a total of 40 ports, of which the stock board can be connected in any combination of the following (up to 40):

- Up to 24 relays for AC outlets
- Up to 8 DC powered devices (12v default, with external power supply 6v-30v)
- Up to 21 digital sensors
- Up to 8 5v/10 PWM or Analog ports
- DS18B20 temperature sensors (multiple sensors technically share a port and can only use one port)
- Up to 4 pH circuits

Hardware Parameter	Minimum	Maximum	Unit
Input DC Voltage	12	20	Volts
Board Current Rating – Standard / Deluxe		7 / 10	Amps
Efficient Reverse Polarity Protection on Input		-24	Volts
Thermal Shutdown Protection on Input		160	°C
Short Circuit Protection on Input		700	mA
Overvoltage Protection *on Input*		20	Volts
Under Voltage Lockout *on Input*	4		Volts
Resettable Fuse on 5v line		2.5	Amps
DC Port Voltage	5	40	DC Volts
Heavy Duty DC Port Current Rating		4	Amps
Standard DC Port Current Rating		2	Amps
Surge Protection on DC Pump Port		125	Amps
Overvoltage Protection on Sensor Ports		500	mW

Figure 10: Board Specifications (Fowler, 2021). The ports sorted by specific connectors is as follows:

- 16 Relays for AC Outlets - two DB9 serial sockets
- 7 Heavy Duty DC Ports - each port has a 2 pin pluggable screw terminal connector
- 1 Auto Feeder Port (standard DC) - uses a 3 pin pluggable screw terminal connector
- 3 Emergency Backup Float Switch Ports - uses a 2 pin pluggable screw terminal connector
- 3 Digital Sensor Ports - each port has a 3 pin pluggable screw terminal connector
- 3 Digital Sensor Ports - uses a USB-A female socket
- 8 Configurable 5v/10v PWM or Analog Ports - uses two 4 pin pluggable screw terminal connectors
- 3 DS18B20 Temperature Ports - 3 use a 3 pin pluggable screw terminal connector, 4 use header pins

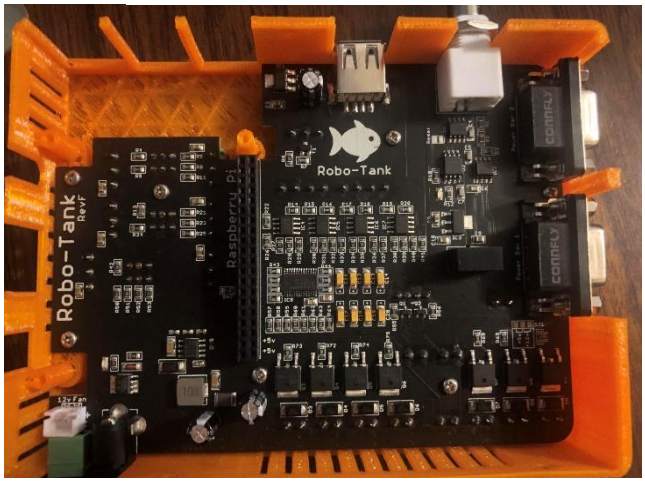

Figure 11: The investigation's Robo-Tank Aquarium Controller (without Raspberry Pi).

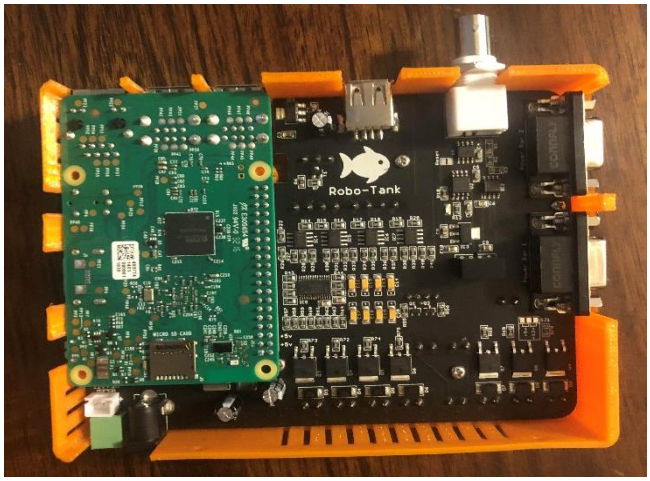

Figure 12: The investigation's Robo-Tank Aquarium Controller (with Raspberry Pi).

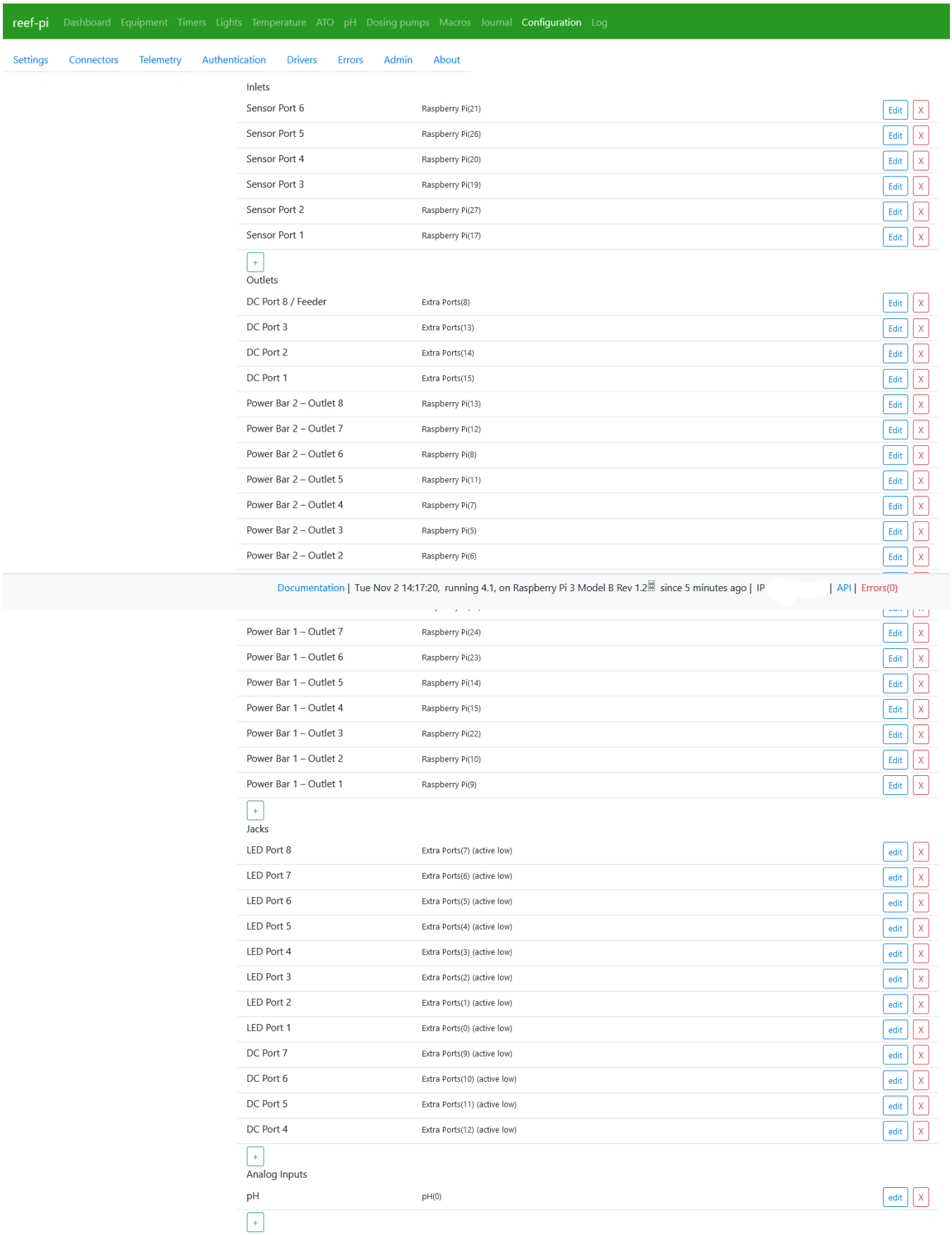

Figure 13: Current Connection Configuration of prototype controller running reef-pi 4.1.

Background

While reef-pi is the software of choice for this project, Robo-Tank Aquarium Controller Software may be a more favorable choice in the future; full functionality of the software includes but not limited to:

Centralized Scheduling System

- Create schedules for AC outlets, DC accessories and dosing pumps
- Schedules can be viewed in an easy to read sort-able and filtered list
- Schedules can run on select days or periodically
- Optional email alerts for each schedule

Custom Rules

- Create custom rules using any parameter
- Custom rules control AC outlets, DC accessories or dosing pumps
- Optional emails when custom rules start
- Add delays so custom rule doesn't run until sensor is stable
- Add delays so equipment doesn't switch immediately
- Override minimum time between doses (preventing accidental overdoses)

Control AC Power Outlets

- Automatic or manual control of each outlet, mix and match
- Lock AC outlet in manual mode and resume to regular mode at later point (remembers manual mode after restart)
- View current status on home page
- Assign custom icons to each outlet (60 icons available)
- Assign custom name to each outlet
- Create multiple schedules for each AC outlet
- Control AC outlets using any sensor with custom rules

Control DC Accessories

- Automatic or manual control of each DC port, mix and match
- Lock DC Accessory in manual mode and resume to regular mode at a later point (remembers manual mode after restart)
- View current status on home page
- Assign custom icons to each DC port, 60 icons available
- Assign custom name to each DC port
- Create multiple schedules for each DC port
- Control DC accessories using any sensor with custom rules

Control Dosing Pumps

- Unlimited dosing pumps
- Dose amounts are in milliliters
- Easy step by step pump calibration system
- Adjust reservoir capacity for each pump
- View total doses remaining in each reservoir on home page and settings page
- Custom color for each reservoir to reflect amount remaining in reservoir
- Pumps won't run when reservoir is empty
- Automatic or manual control of each pump, mix and match
- Control dosing pumps using multiple schedules
- Set minimum time between dosing to prevent accidental over-dosing
- Custom name for each dosing pump
- Control dosing pumps using any sensor with custom rules

Custom Light Modes

- Create unlimited light modes
- Create schedule for each light mode
- Control each channel independently

Monitor Sensors or Switches

- Custom names for each sensor
- All sensors can be used with custom rules to control any equipment

Monitor Multiple pH Probes

- Easy 1 point or 2 point auto calibration wizard
- All probes can be used with custom rules to control any equipment
- Customize name for each probe
- Chart for each probe

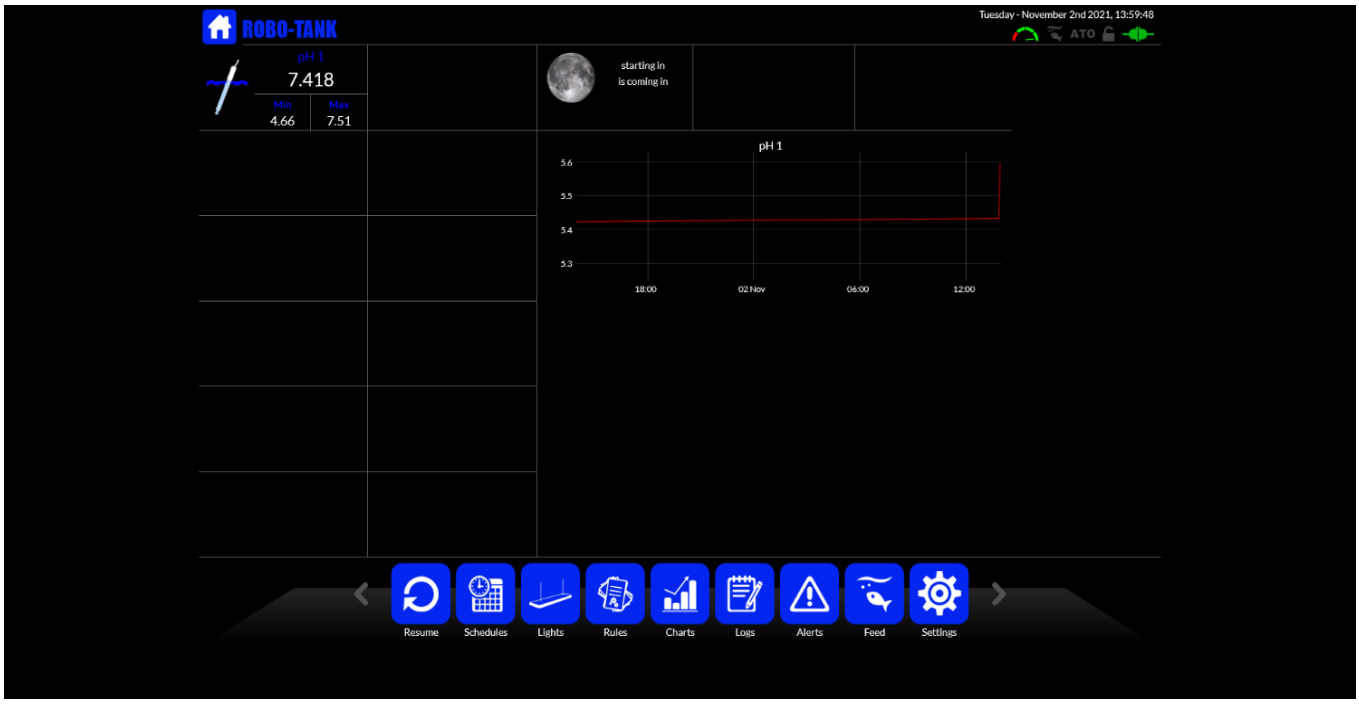

Figure 14: Current Dashboard view of Robo-Tank v6.0 Aquarium Controller Software running on the prototype controller with active pH circuit. It should be noted that at the current time it is not possible to run reef-pi and Robo-Tank software simultaneously.

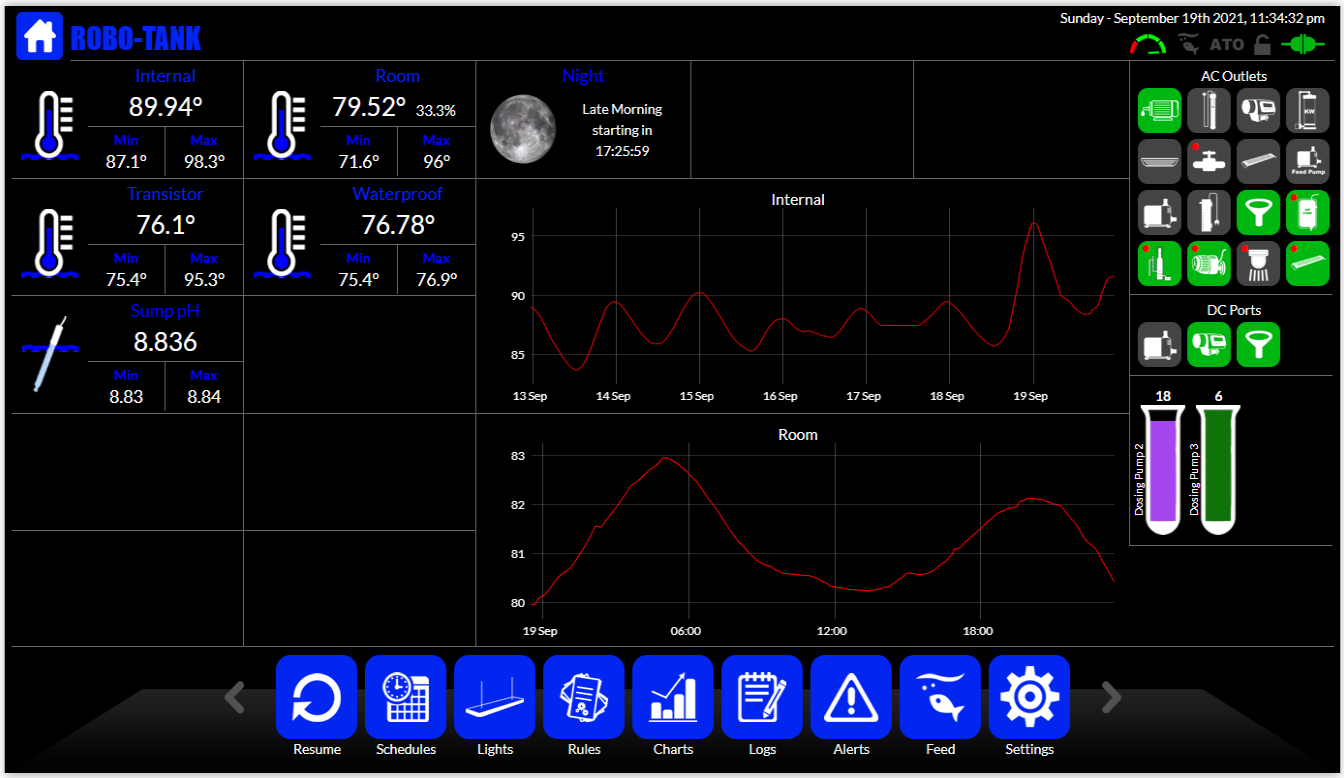

Figure 15: Robert Fowler's Dashboard setup from his Robo-Tank Forum post announcing Robo-Tank v6.0.

Background

In order for tank conditions to be accurately monitored, the following Atlas Scientific embedded circuits have been deployed:

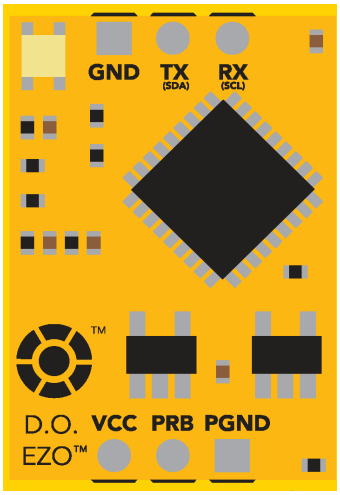

Circuit: Dissolved Oxygen
Range: 0.01 - 100+ mg/L
Accuracy: +/- 0.05 mg/L
Operating Voltage: 3.3V - 5V
Data format: ASCII

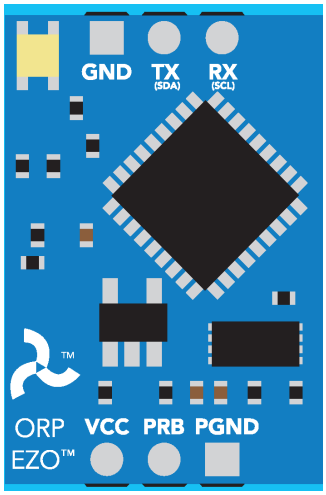

Circuit: Oxygen Reduction Potential
Range: -1019.9mV - 1019.9mV
Accuracy: +/- 1mV
Operating Voltage: 3.3V - 5V
Data format: ASCII

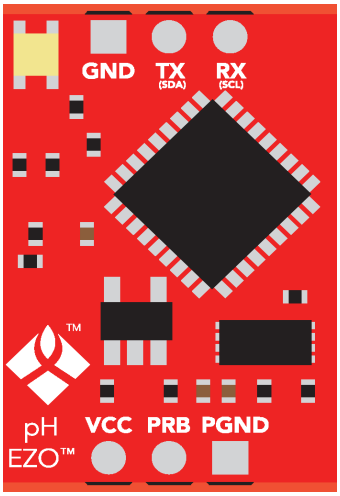

Circuit: pH
Range: 0.001 - 14.000
Resolution: 0.001
Accuracy: +/- 0.002
Operating Voltage: 3.3V - 5V
Data format: ASCII

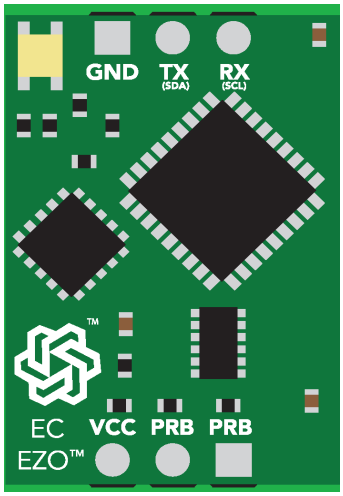

Circuit: Conductivity
Reads: Conducitivy, Total dissolved solids, Salinity, Specific gravity
Range: 0.07 - 500,000+ µS/cm
Accuracy: +/- 2%
Operating Voltage: 3.3V - 5V
Data format: ASCII

Figures taken from Atlas Scientific EZO Datasheets.

Background

Due to the sensitivity of the Atlas Scientific EZO circuits, they are susceptible to electrical noise; electrical isolation is required to prevent rapidly fluctuating readings/consistent inaccurate readings. When dealing with a single circuit, using an inline voltage isolator is sufficient to accomplish this; however, with several circuit working in parallel, it's cost-effective and design-friendly to use a shield. To this end, the Whitebox T1 MkII was included in the build. Originally designed as a Arduino shield, it's capable of interfacing with the Raspberry Pi and can support individual isolation of up to 9 EZO devices. While it can only utilize the I2C communication protocol, it is acceptible in this implementation (the Raspberry Pi 3 doesn't support UART). Furthermore, UART is a disfavorable choice in this instance [it's slow comparitively to I2C and SPI and only supports two devices (in this case, it'd be the Pi and one EZO circuit)].

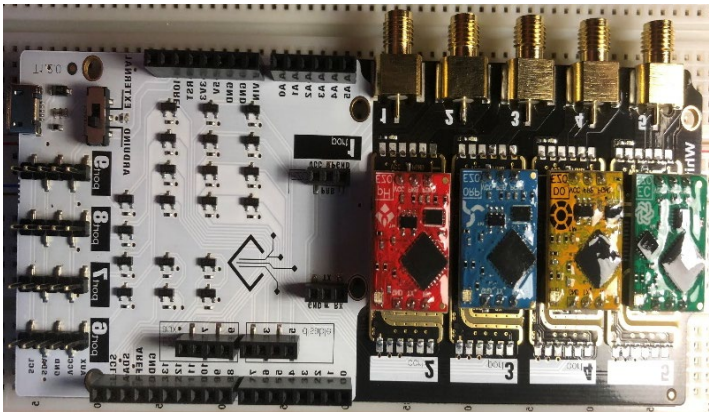

Figure: Whitebox T1 MkII with Atlas Circuit Integration

This is not to say that this methodology is without challenges: Atlas Scientific provides sampling software for sensor monitoring, but that code is not friendly for non-Atlas I2C devices (which the Robo-Tank has in the form of onboard pH circuit and PCA 9685 Expander). The current python script is provided (which has been proven functional for reading circuits on a back-up Raspberry Pi 4 without Robo-Tank integration) and is subject to change. It is the investigation's belief that the scan function within the i2c.py script provided by Atlas that can be modified so that the handling of non-Atlas peripherials is less messy (i.e. the script currently fails to load and exits with an Remote I/O error, an indicator of communication breakdown between perpherial devices and primary computing hub; this should be able to ignored via refinement of the scanning method).

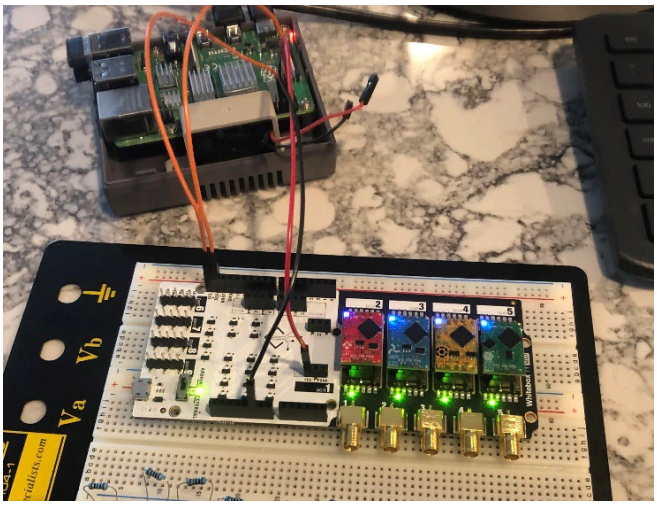

Figure: Operation of Atlas circuits in I2C mode (denoted by blue LED on the top left corner of the chips) with Raspberry Pi 4.

Another way forward could be to forgo using the provided code from Atlas, and to directly add extra ph-EZO drivers into reef-pi for the other circuits. In theory, it should be possible to read from the Atlas circuits with reef-pi: adding a driver and an analog connector using that driver should (after restarting reef-pi) render the circuits readable. This hypothesis is not without detractors; the conductivity circuit is capable of outputing 4 parameters, so it's unclear if reef-pi will only pull in the first (discarding the rest). An additional script will most likely be necessary for this circuit.

Currently, the investigation is working with the developer of Robo-Tank to overcome this hurdle, which has been fully documented on the Robo-Tank Support Forum (so that others looking to engage in similar builds may benefit from the development process).

Background

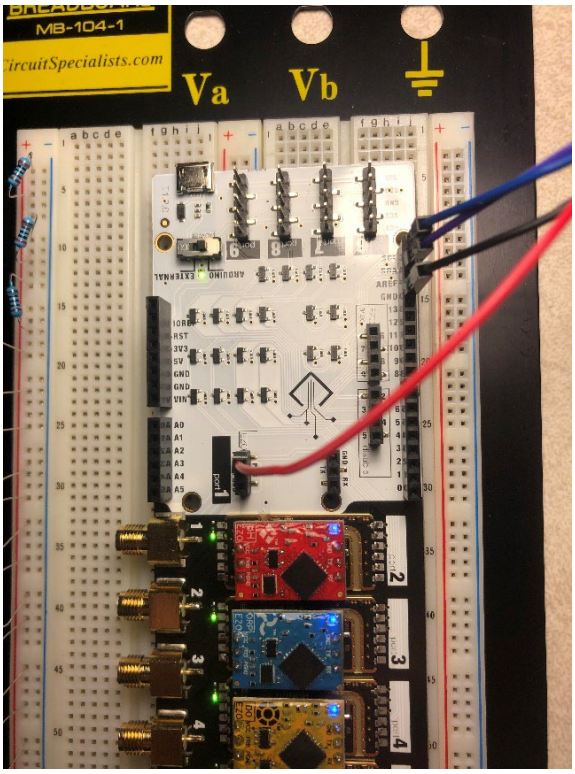

Figure: Top down view of circuit. Wires connected are: 5V power (red), SDA (purple), SCL (blue), and Ground (black).

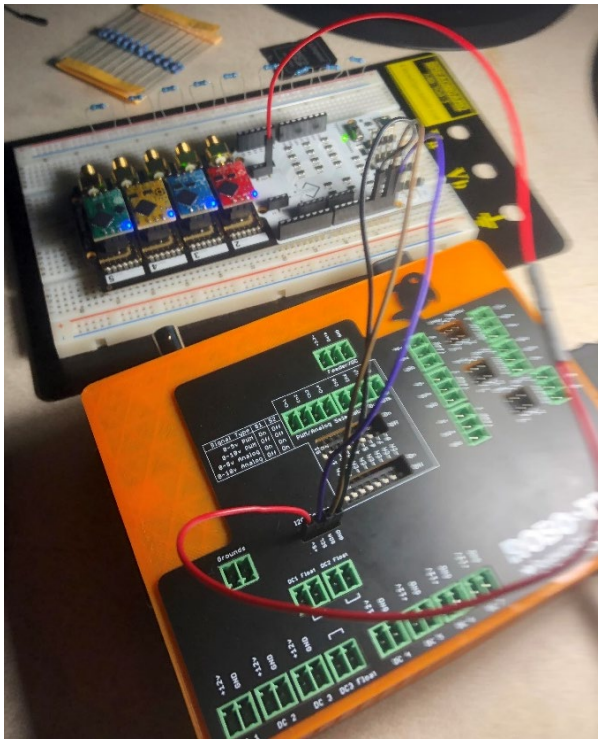

Figure: Robo-Tank successfully powering Whitebox T1 MkII. While Atlas software has so far proven incompatible with the controller, powering the circuit and sucessful identification of circuit addresses is possible with the device.

```
pi@raspberrypi:~/Science/whitebox-raspberry-ezo $ sudo python i2c.py

>> Atlas Scientific I2C sample code
>> Any commands entered are passed to the default target device via I2C except:
  - Help
      brings up this menu
  - List
      lists the available I2C circuits.
      the --> indicates the target device that will receive individual commands
  - xxx:[command]
      sends the command to the device at I2C address xxx
      and sets future communications to that address
      Ex: "102:status" will send the command status to address 102
  - all:[command]
      sends the command to all devices
  - Poll[,x.xx]
      command continuously polls all devices
      the optional argument [,x.xx] lets you set a polling time
      where x.xx is greater than the minimum 1.50 second timeout.
      by default it will poll every 1.50 seconds
>> Pressing ctrl-c will stop the polling

--> DO 32
 - pH 33
 - ORP 34
 - EC 35
>> Enter command: i
Success DO 32 : ?I,DO,2.14
>> Enter command: R
Success DO 32 : 38.30
>> Enter command: 33:status
Success pH 33 : ?STATUS,P,4.02
>> Enter command: R
Success pH 33 : 0.000
>> Enter command: 34:status
Success ORP 34 : ?STATUS,P,3.95
>> Enter command: R
Success ORP 34 : 1016.5
>> Enter command: 35:status
Success EC 35 : ?STATUS,P,3.98
>> Enter command: R
Success EC 35 : 0.00,0,0.00,1.000
```

Figure: Sucessful reading of circuits using Atlas Scientific's sample i2c.py script on the Raspberry Pi 4.

```
Traceback (most recent call last):
  File "/home/pi/whitebox-raspberry-ezo/i2c.py", line 150, in <module>
    main()
  File "/home/pi/whitebox-raspberry-ezo/i2c.py", line 65, in main
    device_list = get_devices()
  File "/home/pi/whitebox-raspberry-ezo/i2c.py", line 26, in get_devices
    response = device.query("I")
  File "/home/pi/whitebox-raspberry-ezo/AtlasI2C.py", line 163, in query
    self.write(command)
  File "/home/pi/whitebox-raspberry-ezo/AtlasI2C.py", line 84, in write
    self.file_write.write(cmd.encode('latin-1'))
OSError: [Errno 121] Remote I/O error
```

Figure: Current error when Atlas Scientific sample i2c.py script is run with the Robo-Tank controller.

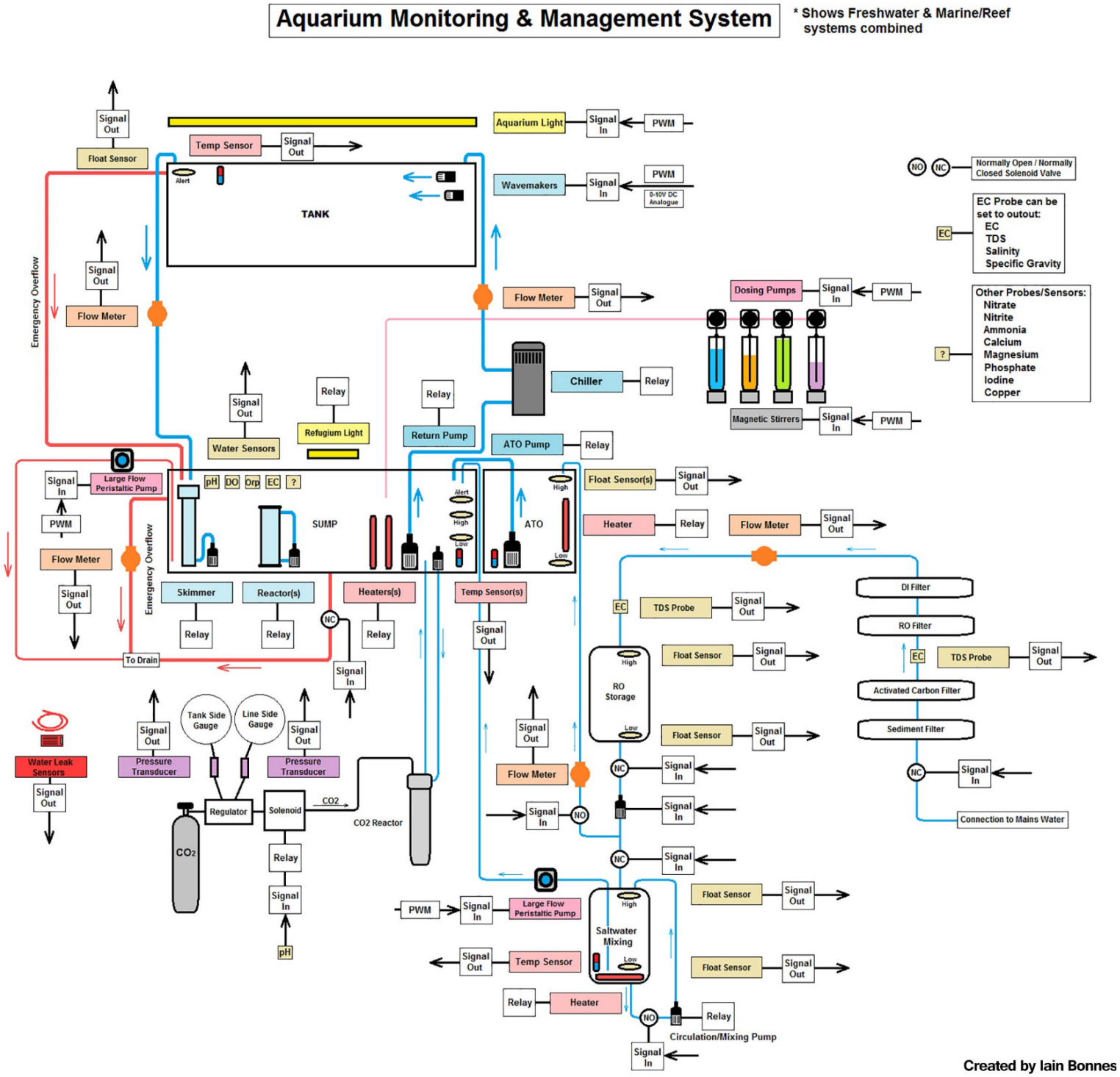

Figure: Complete diagram of fully realized data acquisition and control system (diagram pulled from Robo-Tank Support Forums, developed by Rob Fowler and Iain Bonnes). The investigation will continue development drawing inspiration from this scheme.

Works Cited:

St. Johns River Water Management District, Bethune-Cookman University, Florida Atlantic University-Harbor Branch Oceanographic Institution, Florida Fish and Wildlife Conservation Commission, Florida Institute of Technology, Nova Southeastern University, Smithsonian Marine Station at Ft. Pierce, University of Florida, & Seagrass Ecosystems Analysts. (2012, June). *Indian River Lagoon 2011 Superbloom Plan of Investigation*. St. Johns River Water Management District. https://www.sjrwmd.com/static/waterways/irl-technical//2011superbloom_investigationplan_June_2012.pdf

Lewis, Michael, J. Taylor Kirschenfeld, and Traci Goodheart. Environmental Quality of the Pensacola Bay System: Retrospective Review for Future Resource Management and Rehabilitation. U.S. Environmental Protection Agency, Gulf Breeze, FL, EPA/600/R-16/169, 2016.

Kimon T. Bird, Jewett-Smith, J., & Fonseca, M. (1994). Use of in Vitro Propagated Ruppia maritima for Seagrass Meadow Restoration. *Journal of Coastal Research, 10*(3), 732-737. Retrieved November 24, 2020, from http://www.jstor.org/stable/4298265

Biber, P., Caldwell, J. D., Caldwell, S. R., & Marenberg, M. (2013). Halodule wrightii Propagation Guide. *Coastal Research Laboratory*, 1–6. https://gcrl.usm.edu/cpr/docs/planting.guides/CPR.Halodule.wrightii.pdf

Virnstein, R., Steward, J., & Morris, L. (2007). SEAGRASS COVERAGE TRENDS IN THE INDIAN RIVER LAGOON SYSTEM. *Florida Scientist, 70*(4), 397-404. Retrieved November 24, 2020, from http://www.jstor.org/stable/24321667

Florida Department of Environmental Protection (FDEP) & National Oceanic and Atmospheric Administration (NOAA). (2017, April). *Deepwater Horizon Restoration Project Report: Florida Pensacola Bay Living Shoreline Project* (Portal ID: 26). https://www.google.com/url?sa=t&rct=j&q=&esrc=s&source=web&cd=&cad=rja&uact=8&ved=2ahUKEwib9sK5t5vtAhVXSjABHYNcArAQFjAJegQICRAC&url=https%3A%2F%2Fwww.cityofpensacola.com%2FDocumentCenter%2FView%2F9917&usg=AOvVaw1zIeh1RX4Xv jf-MSalvkpH

One Lagoon & Florida Department of Environemental Protection (FDEP). (2019, August). *FY 2021 EPA Work Plan*. Indian River Lagoon National Estuary Program. https://onelagoon.org/wp-content/uploads/FY2021-EPA-Workplan_Final.pdf

Short, F.T., Carruthers, T.J.R., van Tussenbroek, B. & Zieman, J. 2010. *Halodule wrightii. The IUCN Red List of Threatened Species 2010*: e.T173372A7001725. http://dx.doi.org/10.2305/IUCN.UK.2010-3.RLTS.T173372A7001725.en

Reynolds, L.K., Tiling, K.A., Digiantonio, G.B. *et al.* Genetic diversity of *Halodule wrightii* is resistant to large scale dieback: a case study from the Indian River Lagoon. *Conserv Genet* **20,** 1329–1337 (2019). https://doi.org/10.1007/s10592-019-01214-z

Hall, Lauren & Hanisak, Dennis & Virnstein, Robert. (2006). Fragments of the seagrasses Halodule wrightii and Halophila johnsonii as potential recruits in Indian River Lagoon, Florida. Marine Ecology Progress Series. 310. 109-117. 10.3354/meps310109.

Fonseca, M.S., W.J. Kenworthy and G.W. Thayer. 1998. Guidelines for the Conservation and Restoration of Seagrasses in the United States and Adjacent Waters. NOAA Coastal Ocean Program Decision Analysis Series Volume 12. 222p.

McMillan, C. 1976. Experimental studies on flowering and reproduction in seagrasses. Aquatic Botany 2: 87-92.

McMillan, C. 1981. Seed reserves and seed germination for two seagrasses, *Halodule wrightii* and *Syringodium filiforme*, from the western Atlantic. Aquatic Botany 11: 279-296.

McMillan, C. 1991. The longevity of seagrass seeds. Aquatic Botany 40: 195-198.

Florida Department of Environmental Protection. (2019, February 27). *Project GreenShores*. https://floridadep.gov/rcp/aquatic-preserve/content/project-greenshores

Barnes, R. (2016, February 29). Raspberry Pi 3: Specs, benchmarks & testing. *The MagPi Magazine*. https://magpi.raspberrypi.com/articles/raspberry-pi-3-specs-benchmarks

Fowler, R. (2021, October 9). *Robo-Tank v6.0 is Ready* [Forum Post]. Robo-Tank. https://www.robo-tank.ca/forum/Thread-Robo-Tank-v6-0-is-Ready

Fowler, R. (2020, July 23). *RevB Deluxe Controller DIY Assembly Manual*. Robo-Tank. https://www.robo-tank.ca/Reef-pi-DIY-Hardware/Reef-pi-DIY-Deluxe-Aquarium-Controller-v1

Dey, R. (2021, November 4). *reef-pi :: An opensource reef tank controller based on Raspberry Pi.* [Forum Post]. REEF2REEF Saltwater and Reef Aquarium Forum. https://www.reef2reef.com/threads/reef-pi-an-opensource-reef-tank-controller-based-on-raspberry-pi.289256/

Pensacola, Florida – Naturally Resilient Communities. (n.d.). Naturally Resilient Communities. Retrieved June 11, 2021, from http://nrcsolutions.org/pensacola-florida/

S. Kumar, G. Stecher, M. Suleski, and S.B. Hedges, 2017. **TimeTree: a resource for timelines, timetrees, and divergence times**. Molecular Biology and Evolution 34: 1812-1819, DOI: 10.1093/molbev/msx116.

Lucas, C., Thangaradjou, T., & Papenbrock, J. (2012). Development of a DNA barcoding system for seagrasses: successful but not simple. *PloS one*, *7*(1), e29987. https://doi.org/10.1371/journal.pone.0029987

CBOL Plant Working Group , Peter M. Hollingsworth , Laura L. Forrest , John L. Spouge , Mehrdad Hajibabaei , Sujeevan Ratnasingham , Michelle van der Bank , Mark W. Chase , Robyn S. Cowan , David L. Erickson , Aron J. Fazekas , Sean W. Graham , Karen E. James , Ki-Joong Kim , W. John Kress , Harald Schneider , Jonathan van AlphenStahl , Spencer C.H. Barrett , Cassio van den Berg , Diego Bogarin , Kevin S. Burgess , Kenneth M. Cameron , Mark Carine , Juliana Chacón , Alexandra Clark , James J. Clarkson , Ferozah Conrad , Dion S. Devey , Caroline S. Ford , Terry A.J. Hedderson , Michelle L. Hollingsworth , Brian C. Husband , Laura J. Kelly , Prasad R. Kesanakurti , Jung Sung Kim , Young-Dong Kim , Renaud Lahaye , Hae-Lim Lee , David G. Long , Santiago Madriñán , Olivier Maurin , Isabelle Meusnier , Steven G. Newmaster , Chong-Wook Park , Diana M. Percy , Gitte Petersen , James E. Richardson , Gerardo A. Salazar , Vincent Savolainen , Ole Seberg , Michael J. Wilkinson , Dong-Keun Yi , and Damon P. Little. (2009). A DNA barcode for land plants. August 4, 2009 | 106 (31) 12794-12797 | https://doi.org/10.1073/pnas.0905845106

SWISS-MODEL Workspace:

Waterhouse, A., Bertoni, M., Bienert, S., Studer, G., Tauriello, G., Gumienny, R., Heer, F.T., de Beer, T.A.P., Rempfer, C., Bordoli, L., Lepore, R., Schwede, T. SWISS-MODEL: homology modelling of protein structures and complexes. Nucleic Acids Res. 46(W1), W296-W303 (2018).

Guex, N., Peitsch, M.C., Schwede, T. Automated comparative protein structure modeling with SWISS-MODEL and Swiss-PdbViewer: A historical perspective. Electrophoresis 30, S162-S173 (2009).

SWISS-MODEL Repository:

Bienert, S., Waterhouse, A., de Beer, T.A.P., Tauriello, G., Studer, G., Bordoli, L., Schwede, T. The SWISS-MODEL Repository - new features and functionality. Nucleic Acids Res. 45, D313-D319 (2017).

Bouckaert R., Vaughan T.G., Barido-Sottani J., Duchêne S., Fourment M., Gavryushkina A., et al. (2019) BEAST 2.5: An advanced software platform for Bayesian evolutionary analysis. PLoS computational biology, 15(4), e1006650. https://doi.org/10.1371/journal.pcbi.1006650

Dhar, A., & Minin, V. (2016). Maximum Likelihood Phylogenetic Inference. *Encyclopedia of Evolutionary Biology*, 499–506. https://doi.org/10.1016/b978-0-12-800049-6.00207-9

Brahme, A. (2014). *Comprehensive Biomedical Physics* (1st ed.). Elsevier.

Golding, B., Felsenstein, J. A maximum likelihood approach to the detection of selection from a phylogeny. *J Mol Evol* **31,** 511–523 (1990). https://doi.org/10.1007/BF02102078

Singh, D. B., & Pathak, R. K. (2021). *Bioinformatics: Methods and Applications* (1st ed.). Academic Press. https://doi.org/10.1016/C2020-0-03034-3

Jack Sullivan and Paul Joyce. Model Selection in Phylogenetics. Annual Review of Ecology, Evolution, and Systematics. Vol. 36: 445-466 (2005) DOI: 10.1146/annurev.ecolsys.36.102003.152633

Rambaut A, Drummond AJ, Xie D, Baele G and Suchard MA (2018) Posterior summarisation in Bayesian phylogenetics using Tracer 1.7. *Systematic Biology*. **syy032**. doi:10.1093/sysbio/syy032

Larkum, A. W. D., Kendrick, G. A., & Ralph, P. J. (2018). *Seagrasses of Australia: Structure, Ecology and Conservation* (1st ed. 2018 ed.) [E-book]. Springer https://doi.org/10.1007/978-3-319-71354-0

Papenbrock, J. (2012). Highlights in Seagrasses' Phylogeny, Physiology, and Metabolism: What Makes Them Special? *ISRN Botany*, *2012*, 1–15. https://doi.org/10.5402/2012/103892

Larkum, A. W. D., Orth, R. J., & Duarte, C. (2007). *Seagrasses: Biology, Ecology and Conservation*

[E-book]. Springer Publishing.

Vogl, T., Kickenweiz, T., Pitzer, J. *et al.* Engineered bidirectional promoters enable rapid multi-gene co-expression optimization. *Nat Commun* **9,** 3589 (2018). https://doi.org/10.1038/s41467-018-05915-w

Hollingsworth P. M., Graham S. W., Little D. P. 2011. Choosing and using a plant DNA

barcode. PLoS ONE 6: e1925

Heckenhauer, J., Barfuss, M. H., & Samuel, R. (2016). Universal multiplexable matK primers for DNA barcoding of angiosperms. *Applications in plant sciences*, *4*(6), apps.1500137. https://doi.org/10.3732/apps.1500137

Sievers F, Wilm A, Dineen D, Gibson TJ, Karplus K, Li W, Lopez R, McWilliam H, Remmert M, Söding J, Thompson JD, Higgins DG. Fast, scalable generation of high-quality protein multiple sequence alignments using Clustal Omega. Mol Syst Biol. 2011 Oct 11;7:539. doi: 10.1038/msb.2011.75. PMID: 21988835.

Edgar, R.C. MUSCLE: a multiple sequence alignment method with reduced time and space complexity. *BMC Bioinformatics* **5,** 113 (2004). https://doi.org/10.1186/1471-2105-5-113

FigTree. (2018, November 25). FigTree. http://tree.bio.ed.ac.uk/software/figtree/

Rambaut A, Drummond AJ, Xie D, Baele G and Suchard MA (2018) Posterior summarisation in Bayesian phylogenetics using Tracer 1.7. Systematic Biology. syy032. doi:10.1093/sysbio/syy032

Conrad L Schoch, Stacy Ciufo, Mikhail Domrachev, Carol L Hotton, Sivakumar Kannan, Rogneda Khovanskaya, Detlef Leipe, Richard Mcveigh, Kathleen O'Neill, Barbara Robbertse, Shobha Sharma, Vladimir Soussov, John P Sullivan, Lu Sun, Seán Turner, Ilene Karsch-Mizrachi, NCBI Taxonomy: a comprehensive update on curation, resources and tools, *Database*, Volume 2020, 2020, baaa062, https://doi.org/10.1093/database/baaa062

Waycott, M., Biffin, E., Les, D.H. (2018). Systematics and Evolution of Australian Seagrasses in a Global Context. In: Larkum, A., Kendrick, G., Ralph, P. (eds) Seagrasses of Australia. Springer, Cham. https://doi.org/10.1007/978-3-319-71354-0_5

Lee, H., Golicz, A. A., Bayer, P. E., Severn-Ellis, A. A., Chan, C. K. K., Batley, J., Kendrick, G. A., & Edwards, D. (2018). Genomic comparison of two independent seagrass lineages reveals habitat-driven convergent evolution. *Journal of Experimental Botany*, *69*(15), 3689–3702. https://doi.org/10.1093/jxb/ery147

T. Janssen and K. Bremer, "The age of major monocot groups inferred from 800+ *rbcL* sequences," *Botanical Journal of the Linnean Society*, vol. 146, no. 4, pp. 385–398, 2004.